Digital ignition

&

Electronic fuel injection

By

Richard Bohuslav Kosik

Department of Computer Science and Electrical Engineering

THE UNIVERSITY OF QUEENSLAND

Submitted for the degree of

Bachelor of Electrical Engineering (Honours)

In the division of Electrical & Electronic Engineering

OCTOBER 2000

Richard Kosik

4 Park View Crescent
Shailer Park, 4128
Australia

08 August 2000

The Dean
School of Engineering
The University of Queensland
St Lucia, 4072
Australia

Dear Professor Simmons,

In accordance with the requirements of the degree of Bachelor of Engineering in the division of Electrical & Electronic Engineering, I present the following thesis entitled:-

“DIGITAL IGNITION & ELECTRONIC FUEL INJECTION”

This work was completed under the guidance and supervision of Dr Geoff Walker.

I declare that the work contained in this document is my own, except as acknowledged in the text, footnotes or references, and has not been previously submitted for a degree at the University of Queensland or at any other institution.

Yours faithfully,

Richard Kosik

Aknowledgments

I thank the following people for their contributions to this project:

Dr Geoff Walker, my thesis supervisor for his non-ending commitment and consultation time, also for Geoff's continual suggestions and encouragement towards the project.

Dr David Mee from the Mechanical Department for allowing me to use the VTE-2 VISI-Trainer Engine.

My fellow friends in the solar car room for their support, constant questions, and suggestions.

My parents and family, for their patience during my absences at family outings, and for their continual support.

Abstract

The increasing demand for economy and performance combined with more stringent emissions and legislative requirements has lead to the high level of complexity in engine control modules. Two underlining factors that determine engine performance and economy, are ignition timing and fuel induction. Previous mechanical methods for ignition timing advance and carburetted fuel induction have proven inefficient and unfriendly to the environment. Therefore, the need for precise metering of fuel and split-second ignition timing is of benefit to future human existence on this planet.

In this thesis, a universal ‘digital ignition and electronic fuel injection’ driver was designed, built and tested. The system was tailored to microcontroller and distributor manipulation, to suit both new and old automotive control technologies.

In order to design a digital ignition and electronic fuel injection driver, the principal theory of internal combustion engines, and relevant electrical components is essential. Various engine management systems from Bosch and Jaguar Motor Company are reviewed.

A complete description of the hardware and software is explained, including the reasoning behind crucial design decisions. Where relevant, PSPICE simulations were used in the aid of the determining device characteristics for design strategy.

The project was evaluated and tested on a VTE-2 VISI-Trainer engine, with positive outcomes. It is concluded that the design hardware and software employed in the project perform as required. Finally, recommendations for future thesis avenues of this project are provided.

Table of Contents

Table of Figures

CHAPTER 1

Introduction

1.1 Overview of Engine Management Systems

The increasing demand for economy and performance combined with more stringent legislative emissions requirements has lead to the high level of complexity in engine management systems (EMS). Modern electro-mechanical techniques commonly used in efficiently controlling today's modern cars are techniques that were pioneered on racecars and developed for consumer automotive applications.

The automotive industry supplies a host of advanced technologies all in the name of safety, economy, comfort, and luxury. These advancements include anti-lock braking system (ABS), air bags, traction control, automatic and tiptronic transmission systems. Engine management systems have been developed by a multitude of various companies around the world, all having the same goal; to improve engine performance, better fuel efficiency and reduce emissions. These are all tasks that require full comprehension of the problem and an understanding of how the improvement of one factor can lead to the degradation of another.

The technologies that greatly enhanced performance on modern engines are electronic fuel injection, electronic ignition, and closed loop lambda control together with engine mapping. Electronic fuel injection is a technology that has many advantages over conventional carburetted induction. The benefits start with the superior ability to meter fuel with precise accuracy, and a significant reduction in fuel droplet size. When these benefits are coupled together with an accurate model, the benefits lead to lower running costs.

Electronic ignition is a technology that can allow the spark voltage to be constant for most of the engine rpm range. If used in conjunction with anti-knock control it can greatly increase the lifetime of the engine while providing performance second-to-none. Closed loop lambda control and engine mapping are both technologies that close the control loop, providing precise measurements of fuel passed to the engine. Lambda control works in real time, sampling the exhaust emissions and adjusting the fuel input with the intention of staying within the legislative emission requirements. Engine mapping is a predetermined guide used in conjunction with lambda control to improve engine performance while controlling the volume of emissions released into the atmosphere.

Figure 1 – VISI Trainer

1.2 Thesis Overview

The aim of this thesis is to revise, design and build a digital ignition and electronic fuel injection driver. The hardware should be relatively inexpensive, and must easily connect to various types of engines, making it a universal EMS while providing engine performance second-to-none. The Internal Combustion (IC) engine used is the VTE-2 VISI-Trainer Engine. This engine is a standard 2.6kw 4-cycle engine that as been highly modified. The modifications are a reduction in compression to 2.14:1 to enable a glass head for viewing into the cylinder, while in operation. Plexiglass viewing windows also enable visibility of the camshaft and valve rotation.

The control system presented in this thesis consists of an ignition and injection driver board. Both the ignition and injection driver feature closed loop analogue circuitry. The controller board is a Mitsubishi M16C micro-controller evaluation board with the microcontroller's timers utilized for the metering of fuel and the timing of the ignition. Please refer to Appendix E for complete data on this device. The M16C receives crankshaft position information from the optical position sensor, giving signals every 10 degrees and every top dead center (TDC) or 360 degrees. From this data, respective ignition spark times are calculated and implemented on the coil/plug arrangement.

1.3 Scope of Work for this Thesis

The work achieved in this thesis covers the entire design of hardware and software, from personal computer (PC) simulations to printed circuit board (PCB) development and construction, installation and testing of the ignition and injection driver hardware. High level software C code was written for the controlled operation of ignition and injection for a single cylinder engine. However, important sensory information concerning fuel injection was not practically obtainable due to funding limitations. In this case, estimates were calculated from velocity sensors, where normally sensors would be as data inputs, it should be noted that this is not closed loop control of fuelling. Neither does this provide the benefits of EFI without correct sensory data. For this reason, fuel injection was not implemented on the engine. However, the driver is demonstrated operating an injector coil proving the purpose of this project.

1.4 Outline of Chapter Headings and Contents

Chapter 2 covers the background theory to the internal combustion engine, which is essential to the design processes of this thesis project. The stoichiometric ratio is explained and the importance of controlling the air/fuel ratio, for environmental reasons, is mentioned. The concept of ignition and fuel induction is clarified and an outline of the essential components that can be used in conjunction with micro-electronic controllers to increase engine performance is given. Respective simulation models for the electric / electro-mechanical elements are produced.

Chapter 3 embodies the overview of existing engine management systems (EMS) and their comprising modules. The various components of the Jaguar 4-Litre V8 EMS are outlined, including a historical range of Bosch engine control products.

Chapter 4 gives the hardware design specifications for the project, outlining in detail the reasoning behind project decisions. Both ignition and injection circuit design are discussed, relevant circuit diagrams are given with explanations of their general operation. The ideas and rationale behind certain printed circuit board (PCB) layout techniques implemented in the design are addressed.

Chapter 5 provides a skeletal framework of the software features with an elaborate detail of issues, which effect engine performance. Complete software flow charts were developed to convey the program operation. Finally, a brief description of how to program the microcontroller is specified.

Chapter 6 discusses the performance of the final product as a whole, and of the hardware and software individually. A complete analysis is given of the two hardware modules, outlining the effectiveness PSPICE had in the design processes. Also described are some of the downfalls that were encountered during the process of this thesis project.

Chapter 7 contains the conclusion and pointers to further work on this project.

CHAPTER 2

Background Theory of Internal Combustion Engines

2.1 The Mechanical System

2.11 Operational Concept of the Four Stroke Combustion Engine

The four stroke combustion engine, or the more commonly known spark ignition engine is an internal combustion (IC) powerplant which relies on an externally induced ignition spark to ignite the gasoline-air mixture. Today's four stroke IC engines rely on an intake manifold to mix petroleum with air before introducing this mixture into the combustion chamber during the induction cycle.

The name four stroke IC combustion engine resides from the distinct four stroke operating cycle, which supplies kinetic energy to the crankshaft. The four strokes involve, firstly the induction stroke, secondly the compression and ignition stroke, thirdly the combustion stroke, and finally the exhaust stroke. Induction stroke involves an open intake valve, closed exhaust valve, and the piston travel to be in the downward motion. As the piston moves downwards, it increases the cylinders effective volume. Thus creating a vacuum effect, this draws in the gasoline-air mixture through the open intake valve. The compression stroke sees both the intake and exhaust valves closed, and the piston moving in the upward motion. The upward sweeping motion of the piston, combined with the closure of the valves decreases the volume in the cylinder, thus compressing the mixture within the combustion chamber. The power stroke comprises of a closed exhaust and intake valve, forcing the piston downward due to the rapidly expanding hot gasses produced after igniting the compressed petroleum-air mixture. Finally, the exhaust stroke with a closed intake valve, open exhaust valve, and the piston moving in the upward motion expels the hot gasses from the cylinder chamber. The whole cycle then proceeds to repeat its self again with a new induction stroke. Figure 2 illustrates visually the complete four stroke cycle, and it is seen how one cycle takes 720 degrees to complete which is equivalent to two turns of the crank shaft [7].

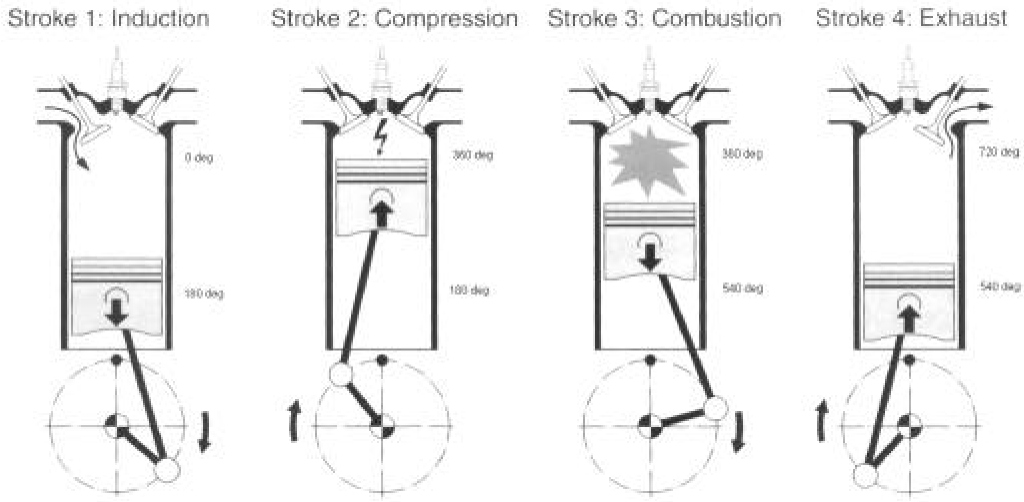

Figure 2 - Operating cycle for a four cylinder engine.

2.12 Air / Fuel Mixture Information

The ideal mixture ratio is known as the stoichiometric ratio or complete combustion ratio. For petroleum, the stoichiometric ratio is at a value of 14.7:1. This means for every 1 kilogram of fuel, 14.7 kilograms of air by weight is necessary for a stoichiometric mixture. When a stoichiometric mixture is achieved all the fuel is burned and emissions are reduced to a minimum. Let us consider now what would happen if the mixture is too rich or too lean. If the mixture is too rich, say a ratio of 13:1 exhaust emissions increase and fuel

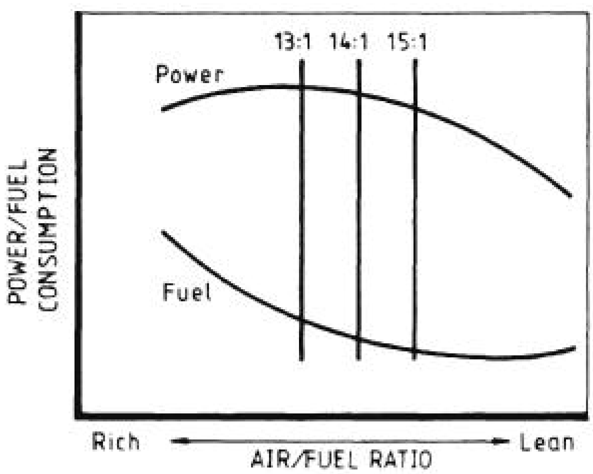

Figure 3 – The stoichiometric air/fuel mixture

consumption rises. If the mixture is at a lean ratio of 15:1 the engine is running most economically and emissions are low, yet power is running at a loss and this may cause engine overheating. Figure 3 depicts the output power and fuel consumption with respect to air/fuel ratio [3].

The by-product of the air/fuel combustion process is CO, HC, and NO_X. To reduce emissions and still have satisfactory engine performance, the air/fuel ratio should be at the theoretical stoichiometric ratio. To provide a satisfactory combustion process precise fuel metering combined with fine mixture vapour are mandatory. If the mixture is not diminutive, then fuel droplets will form along the walls of the inlet manifold, leading to higher HC emissions.

2.13 Ignition: The Concept

Ignition timing is a very important issue, which strongly influences fuel consumption, torque characteristics, and exhaust emissions in the IC engine. The method of ignition has seen many changes over the last twenty years or so. The first systems were coil ignition; this was a complete mechanical system where a solid magnet with its magnetic field excited the coil while passing over it, resulting in the coil firing as the magnetic field collapsed. A number of electro/mechanical designs had made their way into the automotive industry following the coil ignition system; these were the transistorised ignition system and the semiconductor ignition system. Both of these systems have mechanical counterparts, which are somewhat unreliable, as the mechanical sections are prone to fault if not maintained correctly. The distributorless semiconductor ignition, on the other hand, is a complete electric/electronic system less prone to faults than the preceding mechanical counterparts. In figures 4 and 5 below, are the differences between distributor and distributorless ignition systems [14]. It is clear the distributor ignition system has numerous mechanical sections to the design which are prone to failure if not continually maintained, as opposed to the distributorless design which has no mechanical moving sections and requires no maintenance.

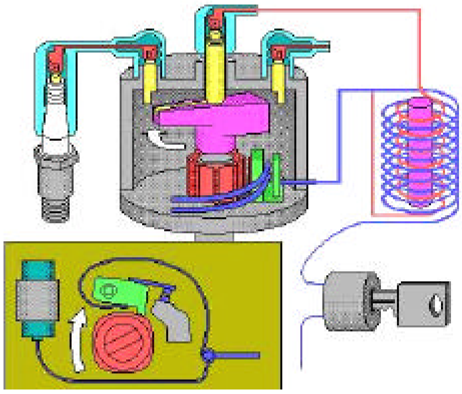

Figure 4 – Distributor ignition

The design of ignition systems for the IC engine depends on the available data for calculating the timing. For instance, the minimum sensor necessary to ignite the spark plug at TDC is an engine cycle sensor. This would give a signal every 720 degrees or once every complete engine cycle. There are equivalent methods, which sense every 360 degrees; these sensors are generally placed on the crankshaft. However, the problem of determining which cycle the engine is in arises. There are two possibilities, depending upon where the sensor is positioned, firstly the engine could be in the induction stroke or combustion stroke. In most cases this does not become a problem as TDC occurs at the same time the induction valve begins to open.

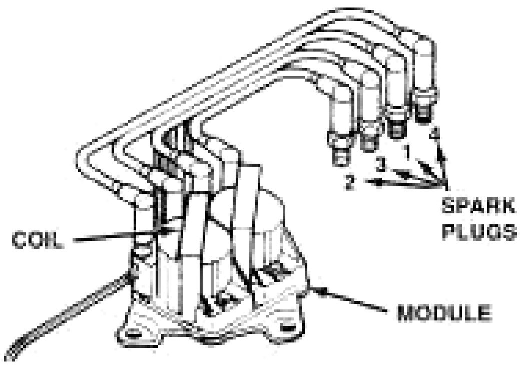

Figure 5 – Distributorless ignition

The variables necessary to calculate sufficiently ignition advance, are engine load and engine speed. Both of these variables can be calculated directly via sensors, one sensing intake manifold pressure, and the other crankshaft velocity. Figure 6 shows the graph known as the ignition advance map, [7]. Every engine has its own advance characteristics, which are determined via dyno testing. This is a map of the ideal ignition angle for the optimal power output with minimal exhaust emissions. Ignition timing also plays a major role in the life expectancy of an engine. Engine knocking is a phenomenon that has plagued engines for many years now. The term knock refers to the high-pressure vibrations that occur inside the chamber when the fuel/air mixture ignites too early. A clear description of this is displayed in figure 7 below [7]. Curve 2 shows the effects of engine knocking on the chamber pressure. These high-pressurised vibrations harm the mechanical components in IC engines and this can lead to premature failure if ignored.

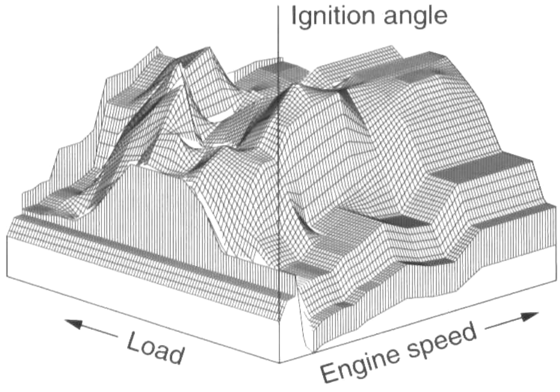

Figure 6 – Ignition advance map

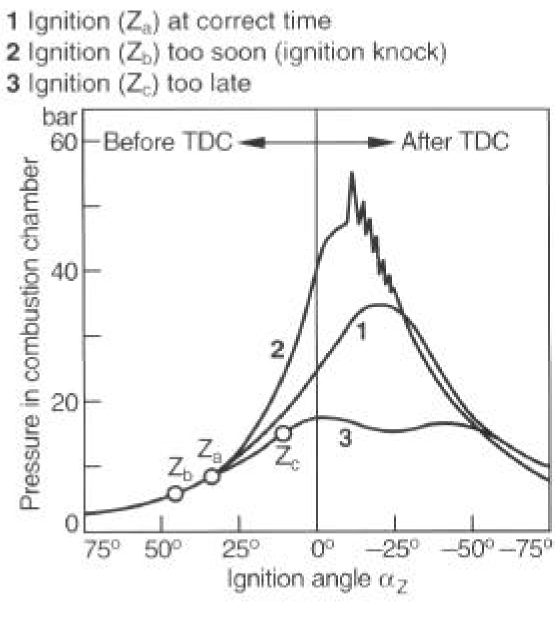

Figure 7 – Combustion chamber pressure

The factors causing knocking could be a rich mixture, while the engine is at high temperature, causing the air/fuel mixture to self-combust. There is a trade-off to the extent of which knocking is deemed acceptable. To run an engine at high-performance, ignition is normally performed close to the detonation limit in order to improve fuel economy and increase power output. With a knock sensor placed on the cylinder head it is possible to sense for knock occurrence. If knocking is over a preset limit, the EMS can then retard the ignition timing to the particular cylinder affected.

It is imperative to know the maximum time between ignition sparks for an engine so a design can provide constant spark energy over a complete engine operating speed. If we take a single cylinder engine at 10,000rpm for example, the time between ignition sparks is T = 1/(rps/2). The factor of two comes from the fact that there is one spark per engine cycle or 720 degrees, but the engine speed is given with reference to 360 degrees. As rps is equivalent to Hertz, time T = 1/freq in seconds. The delay time between sparks, for a single cylinder engine, is then rps = 10,000rpm/60 = 166.66rps, T = 1/(166.66/2) = 12msec. The same calculation for an engine operating at idle (800rpm) yields rps = 800rpm/60 = 13.33rps, T = 1/(13.33/2)= 150msec. Now with the fastest ignition interval being 12msec an ignition system can be designed to these specifications.

2.14 Fuel Induction into the Cylinder

This section plays a major role on the fuel efficiency, the engines starting performance, overall engine performance, and the ability to control the effects of knocking in each cylinder. Today's efficient engines use fuel injection technology, rather than inefficient carburettors.

Carburettors are a mechanical system that mixes fuel with air. To accomplish this, carburettors use what is known as the venturi-effect. Carburettors, as in figure 8, work on the principle of pressure difference sucking the fuel through a miniature tube, which releases small droplets of fuel into the air. The first disadvantage of this system is the restriction in the air passage to the cylinder that produces the necessary pressure difference. Secondly, the fuel droplet size is relatively large when compared to what can be achieved with fuel injection. This system was very popular in the past, however since the development of the fuel injector solenoid, fuel injection has become a more popular method of induction.

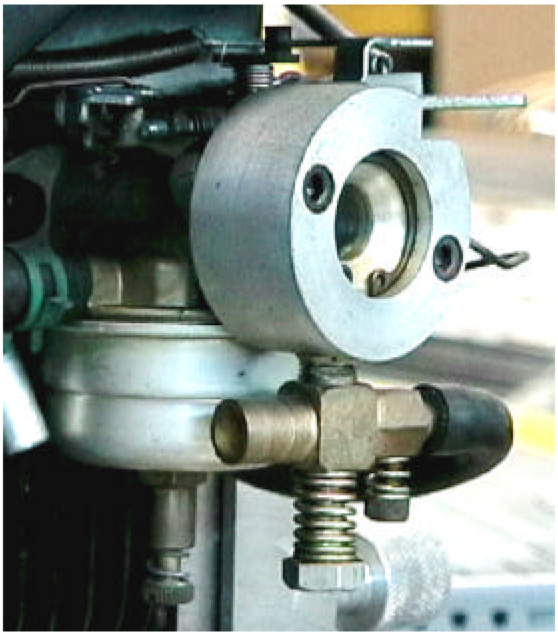

Figure 8 – Carburettor on VISI-Trainer

The fuel injector solenoid can be simply described as a logic tap system. Hence the injector either allows fuel to flow at a fixed flow rate, or not at all. As the injector changes from one state to another, there is some non-linear flow characteristics, however this is quite normal.

There are several possibilities of fuel induction that have been used, all having their own reason or purpose for using that method. The different methods of induction are as follows, from most primitive to most recent: carburettor, throttle body injection (TBI), multi-point injection (MPI). The two last systems mentioned are the fuel injection methods. From these, the MPI is the most expensive to implement, as it requires one injector solenoid for each cylinder. TBI on the other hand only requires one injector solenoid for a multitude of cylinders. The advantages of MPI outweigh the effect of implementation costs in automobiles. With such a system, the injectors can be positioned to channel their spray directly into the intake valve, thus reducing the possibility of fuel touching the chamber walls. The major issues for using multi-point fuel injection over carburettors or throttle body are lower exhaust emissions, better fuel efficiency, increased engine performance and individual fuel control into each cylinder (thus decreasing the effects of knocking). In figures, 9 and 10 below are the illustrations of how TBI and MPI are implemented on the intake manifold [14].

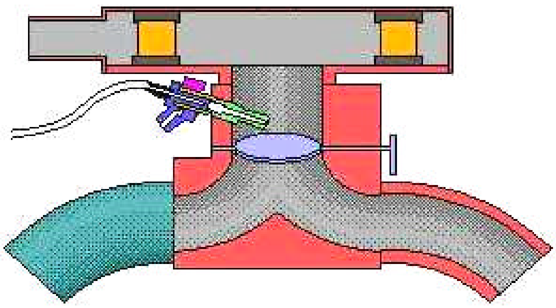

Figure 9 - Throttle body injection

As mentioned earlier, to increase fuel consumption and lower exhaust emissions, it is ideal that all of the fuel expelled from the injector is channelled into the combustion chamber. During the fuel/air mixing phase, if the minute fuel droplets make contact with the manifold walls, they will stick to the walls until enough liquid has built up for the fuel to slide down the manifold walls into the intake valves. When the valve next opens, the large droplet of fuel passes through to the chamber. However, the fuel droplet does not completely ignite because of its size, thus the remnants exit the engine, increasing exhaust emissions.

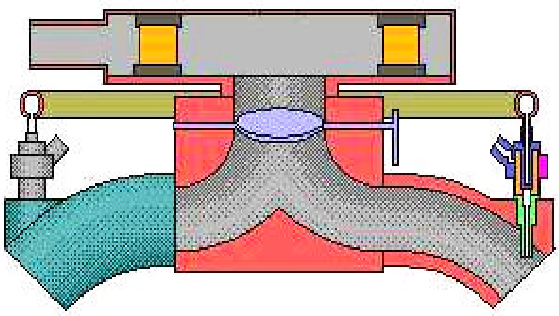

Figure 10 – Multi point injection

Fortunately, the phenomenon described above can be reduced to a point where it can be deemed insignificant. This involves the appropriate selection of injector solenoid. Figures 11 and 12 show two styles of injector spray patterns that are readily available [6]. The simplest and first injector built was the conical spray design. In this style of injector, various values of α can be achieved, giving different results on the quality of air/fuel mixing. The dual spray design was implemented to improve the quality of air/fuel mixing thus having a uniform mixture in the chamber.

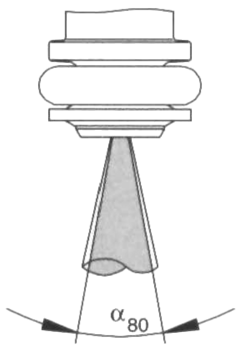

Figure 11 – Conical spray

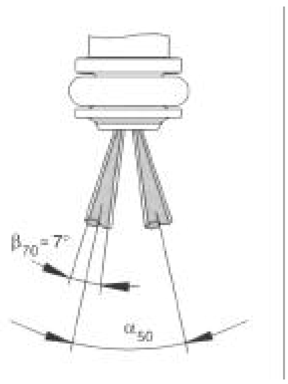

Figure 12 – Dual spray

2.2 The Electrical / Electronic System

2.21 Ignition Coils

Conventional coils used in earlier model automobiles utilised larger cylindrical coils in conjunction with distributors. The secondary winding on these coils are wound directly onto the laminated iron core and connected electrically to the centre tower in the cap of the ignition coil. Since the high-voltage is applied to the core, the core must be insulated by the cap and an additional insulator inserted in the base. The primary winding is located near to the outside around the secondary winding. The primary current, which is switched on and off by a switching device (maybe a distributor, Darlington transistor, MOSFET or IGBT, depending on the application) flows through the primary winding. As the switch is turned on, current flowing through the primary winding causes a magnetic field that magnetises the iron core. When the switch opens its contact, the voltage flips from positive-negative to negative-positive. In doing so, a voltage spike is induced on both primary and secondary side.

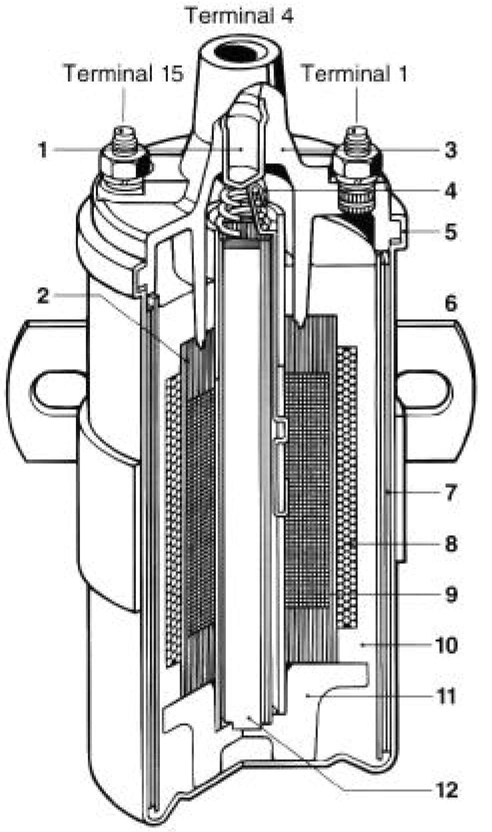

1 High-tension connection on the outside, **2** Winding layers with insulating paper, **3** Insulating cap, **4** High-tension connection on the inside via spring contact, **5** Case, **6** Mounting bracket, **7** Metal plate jacketing (magnetic), **8** Primary winding, **9** Secondary winding, **10** Sealing compound, **11** Insulator, **12** Iron core.

Figure 13 – Ignition coil structure

Previous studies have shown that stoichiometric composition mixtures require a minimum of 0.2mJ of electrical spark energy for ignition to occur. For rich or lean mixtures, the minimum electrical spark energy is 3mJ. If insufficient electric spark energy is available then ignition does not occur. This causes misfiring, which degrades performance and increases exhaust emissions. This is why adequate spark energy is important to ignite any mixture during the worst-case scenario. The appropriate equation for stored energy in an inductor is $W_s = \frac{1}{2}(L_p)(i_p^2)$, in Joules, where L_p is the primary inductance of the autotransformer in Henries, and i_p is the current flowing through the primary winding in Amperes.

A typical ignition coil, as in figure 13, has a turns-ratio of primary to secondary winding 1:100 [7]. The primary resistance and inductance determine the amount of stored energy, while the secondary inductance determines the induced voltage, spark characteristic, and spark duration. Another important factor is the value of coil resistance, as this effects the rate of charge possible for the ignition coil. Low internal resistance is advantageous, as faster charge rates and high output voltages are achievable. Ignition coils, or autotransformers can be modelled via a series resistance R1 representing the coil resistance on the primary side, and R2 representing the coil resistance on the secondary side. Shown below, in figure 14, the two resistors are coupled via transformer TX2 with coupling core between the two coils.

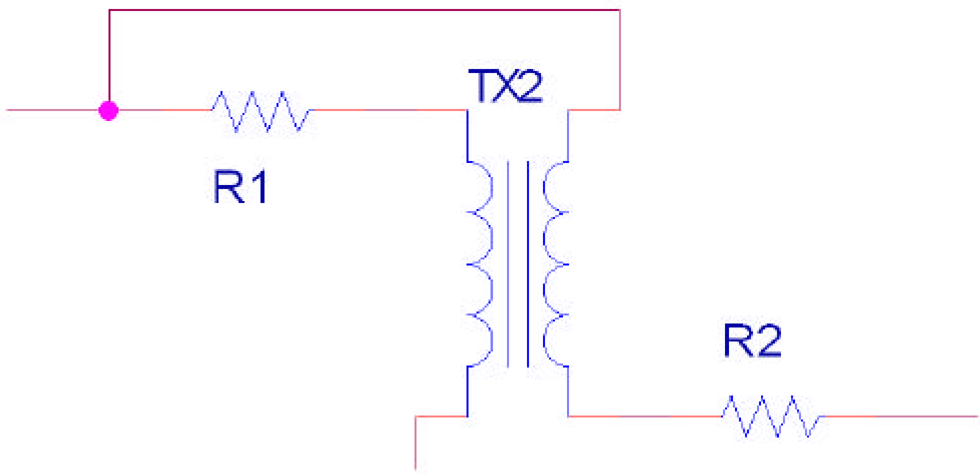

Figure 14 – Equivalent ignition coil model

Knowing primary coil rise time becomes important when calculating what spark frequency the ignition coil can operate to. For example, when an engine is running at 10,000rpm, the issue arises of whether the ignition coil is capable of supplying the same spark energy to the plug as when the engine is running at 800rpm. If the rise time of the coil is not fast enough to charge the coil fully at the higher rpm, then the stored energy in the transformer core will not be sufficient enough to ignite the mixture in the chamber. An appropriate model for the autotransformer primary side enables the calculation of the coil's rise time, and hence the maximum spark frequency can be determined. From the ignition coil equivalent model, the primary side model is just the resistor R1 in series with the inductor L1 as illustrated in figure 15.

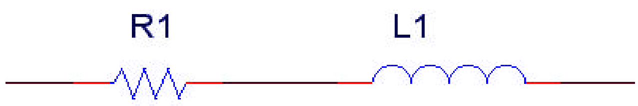

Figure 15 – Equivalent ignition primary side model

2.22 Fuel Injector Solenoids

The electric fuel injection solenoid precisely meters the amount of fuel entering the combustion chamber. This is achieved via fluid flow calculations and precise timing. For example, if you were to measure the amount of fluid γ, in cubic centimetres (cc) that passes through the injector solenoid over a span of one minute, while the inlet fluid pressure into the solenoid was regulated at constant pressure δ, then the flow rate of the injector solenoid, at fixed inlet pressure δ, is known. The flow rate would then be the quantity of fluid γ divided by the time

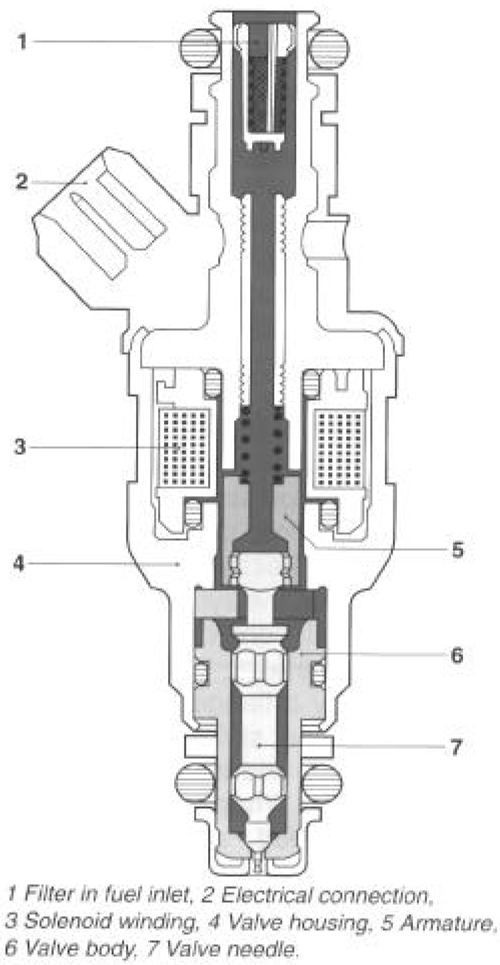

Figure 16 – Injector solenoid

the solenoid was open, one minute, thus $FL_{rate} = \gamma$ in cc per minute.

The injector solenoid, in figure 16, consists of a valve body and the needle valve with fitted solenoid armature [6]. The valve body contains the solenoid winding and the guide for the needle valve. When there is no current flowing in the solenoid winding, the valve needle is pressed against its seat on the valve outlet by a helical spring. When current is passed through the solenoid winding, the needle valve is lifted from its seat and the fuel can stream through the annular orifice. The rise time of the injector valve is important when calculating the amount of fuel to be injected into the chamber. This is particularly true because the fuelling equation will need to take this rise time factor into consideration and suitable flow rate compensation will be necessary during the transition from fully closed to fully open. Typical rise times are in the order of 1msec to 1.5 msec depending on the RL circuit values of the injector and downward force of the spring.

Fuel injector solenoids can be modelled as a resistor R1 in series with an inductor L1. Figure 17 represents an equivalent electrical circuit model of an injector solenoid.

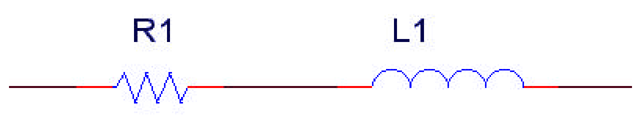

Figure 17 – Equivalent injector circuit model

Standard Ohms law $V = IR$ applies here as well as ideal inductor equation

$V = L(di/dt)$ and power equation $P = VI = LI(di/dt)$.

CHAPTER 3

An Overview of Existing Ignition & Fuel Injection Systems

3.1 Overview of a Commercial Engine Management System

The Engine Management System (EMS) controlling the Jaguar 4-Litre V8 engine, known as the AJV8, is a complex yet versatile piece of engineering [1]. This system controls fuel injection, ignition timing, closed loop fuelling, also controlling an electric throttle body, knock sensing, variable valve timing, engine cooling fans, and high-speed real-time serial communications using 'computer area network' (CAN) protocol to manage traction control and automatic transmission systems.

The closed loop EMS calculates variables detected via the various input sensors on the engine and then sets the completely separate timer module that runs the engine. Every new scan cycle of the program, new variables are calculated. If change has occurred from the previous cycle, the timer module will be updated. A sophisticated on board diagnostics (OBD) system monitors the engine sensors and actuators to determine a fault, if one were to occur.

The Jaguar EMS has a 50% coding split reserved for OBD. This is particularly important as faults could prove to be disastrous.

The EMS consists of two 16 bit Motorola 68HC16 microprocessors, each with a memory capacity of 96kB operating at a clock speed of 16MHz. A backup IC is included as a means of drivability if the main microcontroller were to malfunction. When a failure occurs, it is helpful to know the engine variables and the sensors state at the time of the failure. This can help determine the cause of the problem. The program stores the failure type with freeze frame sensor data at the time of the failure. Input sensors are continually analysed against known correct values for open and short circuit diagnostics. Correct known values are determined via theoretical analysis and practical testing. Various factors including ambient temperature and atmospheric pressure are given specific ranges of operation against expected engine and vehicle running conditions.

Actuator failure is determined via additional monitoring circuitry for failure diagnostics. The diagnostics circuitry can simply consist of a feedback comparator, measuring the output driver and testing it with the desired operating point. If they are not equal, a fault has occurred. Using these fault detection methods, the chance of a disaster is greatly reduced as additional coding can be implemented to shut off certain cylinders (or the whole engine, if necessary) to eliminate the destruction of the engine.

3.2 Bosch Systems

The well-known company Bosch, has developed a series of engine ignition and fuel injection systems, incorporating closed loop control into some later microcontroller designs. The variety of designs carried out by Bosch automotive division is rather extensive, in all cases providing innovative technology to the automotive environment for the particular time the design was released. The table in figure 18, illustrates the component sections for the different ignition designs proposed [7]. Moving from left to right, the table begins with the first ignition system to the most recent and advanced system available on the market today. The system provides the following advantages over other systems;

- Lower electro magnetic interference.
- No rotating components, leading to higher system reliability.
- Ease of manufacturing.

Function	Ignition system			
	CI	TI	SI	DLI
	Coil ignition	Transistorized ignition	Semiconductor ignition	Distributorless semiconductor ignition
Ignition triggering (pulse generator)	mechanical	electronic	electronic	electronic
Determining the ignition angle on the basis of the speed and load condition of the engine	mechanical	mechanical	electronic	electronic
High-tension generation	inductive	inductive	inductive	inductive
Distribution and assignment of the ignition spark to the correct cylinder	mechanical	mechanical	mechanical	electronic
Power section	mechanical	electronic	electronic	electronic

Figure 18 – Bosch ignition system definition table

Bosch's first ignition method was the coil ignition system (see figure 19, below) [7]. This system was a mechanical feat at the time, requiring no fixed magnets and providing mechanical advance, the first for the time.

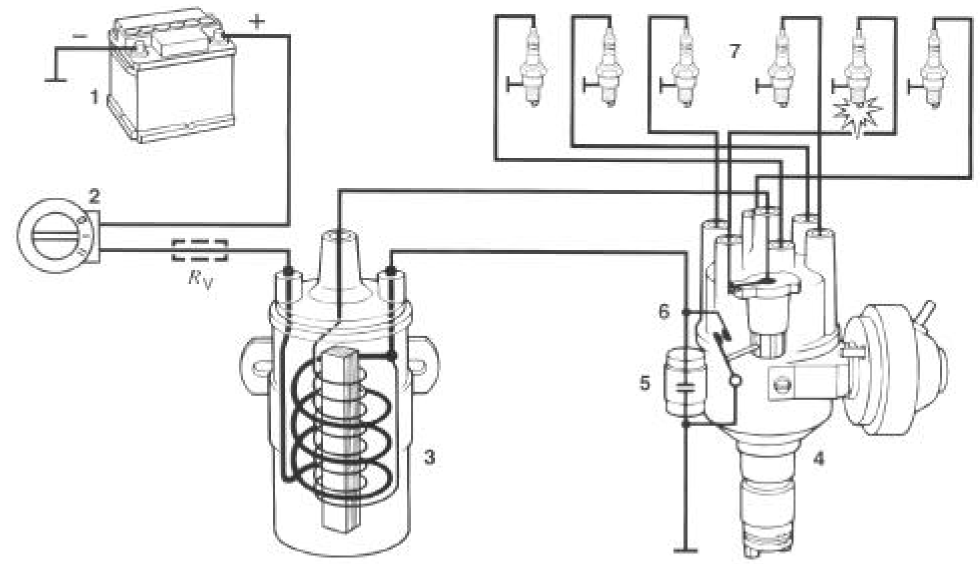

Ignition system with conventional coil ignition

1 Battery, **2** Ignition and starting switch, **3** Ignition coil, **4** Ignition distributor, **5** Ignition capacitor, **6** Contact breaker, **7** Spark plugs, R_V ballast resistor for boosting the starting voltage (not always fitted).

Figure 19 – Bosch coil ignition system

Some of the hardware that was included in the designs of the time is reproduced in black and white in figure 20, [7]. This illustrates the prime of semiconductor ignition systems that were introduced at the time. Systems like this one include electronic advance, knock control, and engine map storage capabilities. The printed circuitry board (PCB) technology was preceded with predominantly surface mount device (SMD) components, leading to the ease of manufacturing.

Equally, the injection circuit PCB is of similar standard to that of the ignition module. A picture of the Bosch L-Jetronic controller module is represented in figure 21 [6].

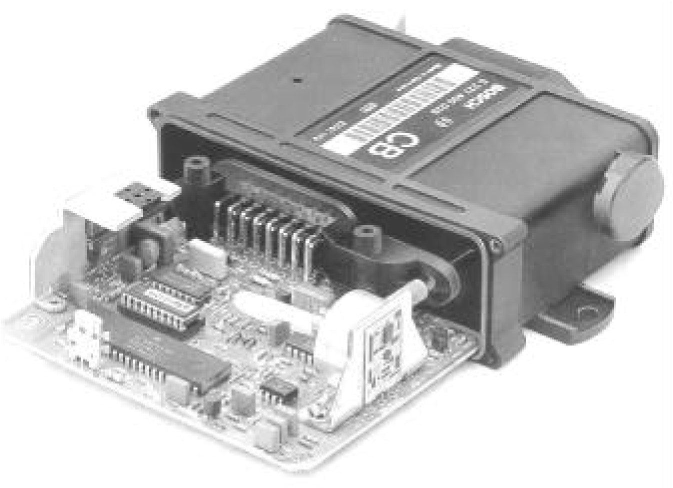

Figure 21 – Bosch ignition module

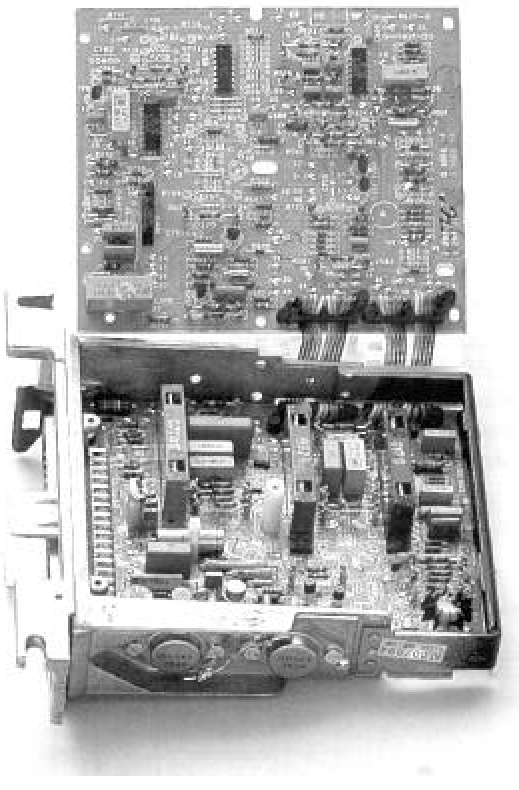

Figure 20 – Bosch L-Jetronic controller

CHAPTER 4

Hardware Design & PSPICE Modelling

4.1 Specifications

This digital ignition and electronic fuel injection was designed to be universal, so it could be ported to any engine while being fully configurable for standard ignition and injection elements, as well as performance components. The ignition and injection driver must have the following features:

- Adjustable current limiting through the ignition coil.
- Adjustable max current limit through the injector coil.
- Adjustable hold current through the injector coil.
- Relatively simple, inexpensive to manufacture, with minimal component count.

The system should also be easy to integrate to different control modules, for example; could be controlled via microcontroller or older distributor systems as well.

4.2 Circuit Design

There are two major options to the operation of this system. Firstly, the features mentioned above could be integrated into a microcontroller-based system, although this may be rather costly if it could be achieved via analogue circuitry. The analogue circuitry consists of an operational amplifier being used as a comparator stage, controlling the flow of current through the coil. The implementation cost of a system like this would be far more economical than a microcontroller system. The benefits of such a system include no programming of microcontrollers, hardware is less expensive, and users could easily adjust limits to their system via potentiometers.

4.21 Ignition Circuit

The ignition coil chosen for the project, was a high-performance coil manufactured by Robert Bosch in Australia. The MEC717 coil, as labelled on the packaging, is a 12 volt coil with low primary resistance of 1 Ohm and coil inductance of L_p = 2.58mH by inspection. A safe ignition energy value of 20mJ, for a spark to occur under all conditions, is selected. To calculate the necessary

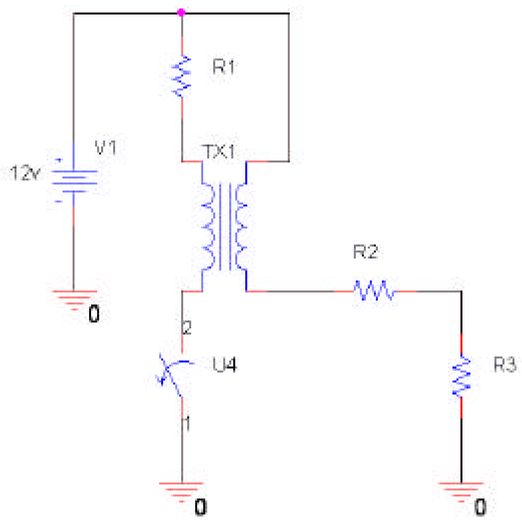

Figure 22 – Ignition circuit model

current through the coil, the equation $Ws = ½(L_p)(i_p^2)$ is used, where Ws = 20mJ and L_p is known. Then i_p^2 is calculated to be 40/2.58 = 15.5 and i_p is $\sqrt{15.5} = 3.94A \approx 4A$, therefore roughly 4A is required to flow through the primary winding to produce an energy level of 20mJ in the coil.

Figure 22 is a respective model of an ignition circuit. R1 and R2 represent the winding resistance for primary and secondary coils, and R3 represents a high resistance spark gap of air. (R3 does not correctly model a spark gap, yet this is however not the issue being raised.) Switch U4 closes the current loop for the primary winding, allowing the core to be magnetised. As U4 open circuits, the voltage across the primary coil inverts, causing a large voltage spike, which is passed through to the secondary coil, causing a spark across the spark plug. The large voltage spike evident on the secondary coil is also present (in smaller magnitude) at the switch U4 on the primary coil. There is a compromise as to how large a voltage spike can be produced on the output coil, because of the proportionality with voltage levels at the switch, not to mention issues of electro magnetic interference (EMI), that can affect every piece of electronic circuitry in the automotive environment.

The large voltage spikes present on the secondary coil when the switch is turned off are also present at the primary coil, with different magnitude. This can become a problem for a semiconductor-switching device. Different types of semiconductor switches have different resistance to high-voltage spikes. The types of semiconductor switching devices considered for the circuit, to name a few, are; Thyristor, BJT, Darlington transistor, MOSFET, and IGBT. From these devices the switches with highest resistances to voltage transients (in order from highest to lowest) are; Thyristor, IGBT, Darlington transistor, BJT, MOSFET, with the last three devices having very similar high-voltage resistances. Thyristors and IGBTs are best suited to the high-voltage characteristic and cost effective demands. However, it is possible to select MOSFET's that will sufficiently handle the high-voltage demands, but these are several times more expensive. As the switching device must be able to limit the current through the ignition coil, the use of a Thyristor is unquestionable, with its inability to turn off on demand. The IGBT is perceived as the best-suited semiconductor-switching device, considering cost and functionality for this application.

Having chosen the switching device for this application, the switch, U4 in figure 22, can now be replaced with the equivalent model IGBT. The IGBT used in this design was the SGP10n60, manufactured by Infineon Technologies. Please refer to Appendix D for complete data on this device. The next important matter to look at is the rise time of the primary coil and switch to determine the time for i_p to reach 4A, from an initial open circuit. By doing this, it is possible to find out two things; firstly what the maximum spark frequency is, while delivering 20mJ of energy; secondly, in a timed based control system, like a microcontroller system, the delay time for the current to build up to 4A can be incorporated into control calculations. Thus, minimising the power that would normally be dissipated in the form of heat, for a distributor control system. The model, which can be used for determining the rise time, is shown in figure 23. V2 is used in this instance to drive the IGBT gate on and off. When this circuit is simulated in OrCAD - PSPICE, the following rise time was observed, as portrayed in figure 24. It is visually evident here that the delay time for 4A to be reached is roughly 1.25msec. From this, it is possible to calculate the amount of power loss for a time based control system, assuming the turn-on time is 1.25msec. Determined from the data sheets, the voltage across the IGBT switch at 4A is 1.5V, so P = IV(D) where D is the ratio of time the switch is on divided by the time it takes to complete one engine cycle at

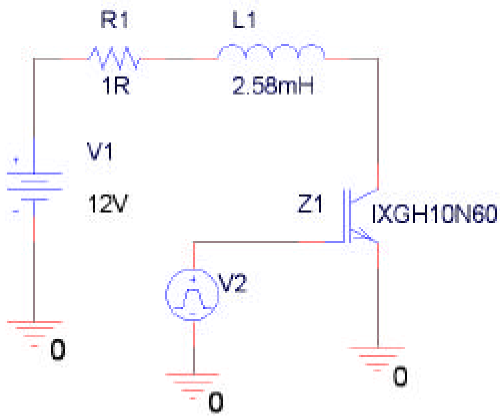

Figure 23 – Coil rise-time model

10,000rpm, D = t_{on}/t_{cycle} where t_{cycle} = 12msec. This calculation only gives the maximum possible power dissipation. The actual power loss would be several times less. The calculation is ⇒ P = 1.5 x 4 x (1.2/12) = 0.6W worst case scenario for a time based control system. Equally, the power dissipation for an engine at idle (800rpm) is ⇒ P = 1.5 x 4 x (1.2/150) = 0.048W. It is clear that the IGBT would not need to be mounted to a heatsink (operating in the ohmic region reduces power dissipation) for this proposed design. However, were the ignition circuit controlled via a distributor, where precise values of t_{on} = 1.2msec are not realistic (anywhere in the area of > 5msec), the power dissipation of the switching device will rapidly increase. In this case, a heatsink would be necessary as the device would be using the current regulation circuitry, thus the IGBT would be operating in the active region of the component.

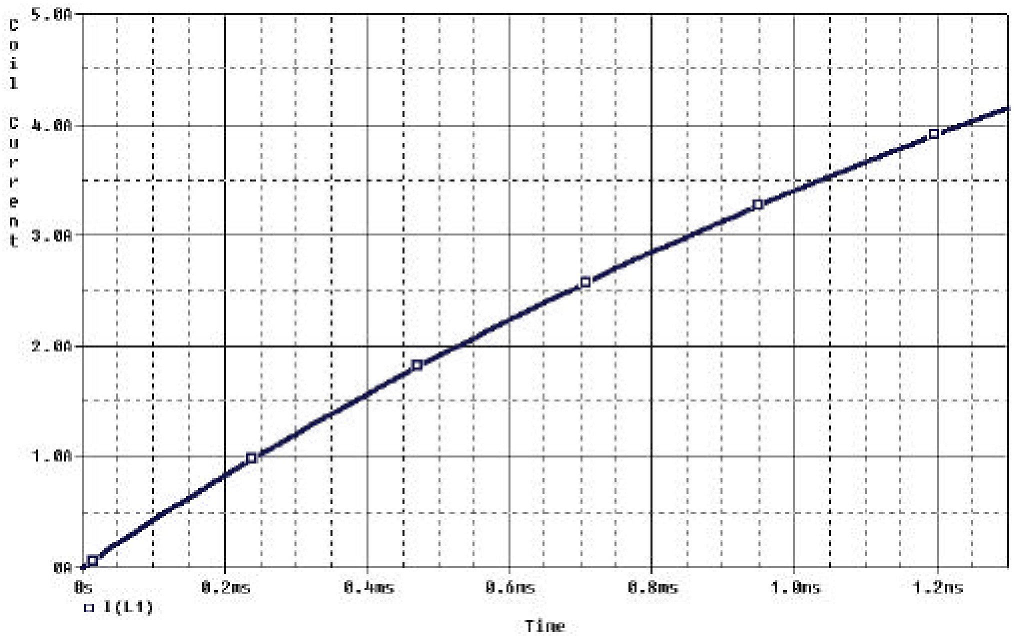

Figure 24 – Rise-time of primary coil current

To limit the current in a distributor control system, the control loop for the IGBT needs to hold the current at 4A until such time when the coil will be fired. For this type of system the controller necessary is that shown in figure

25. From the diagram, a measure of output current needs to be fed into the controller, as well as the reference current level. The control loop is implemented electronically via an operational amplifier configured as a differential amplifier, which controls the IGBT.

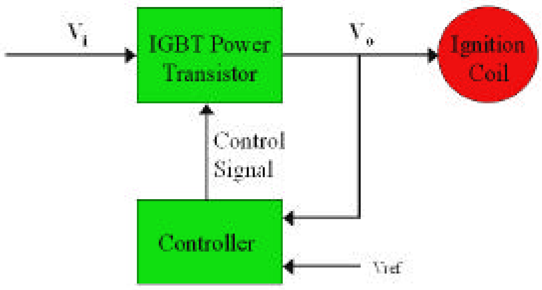

Figure 25 – Ignition control loop

The amplifier incorporated in the control circuit is a general-purpose single supply operational amplifier, the LM324. This op-amp is manufactured by National Semiconductor, for a more complete data specification please refer to Appendix E. The differentiator circuit appears in figure 26. The reference voltage is on the positive input of the amplifier, and its voltage level is adjusted via P4. Both C5 and C4 operate as smoothing capacitors to eliminate any voltage spikes that may interfere with the op-amps response.

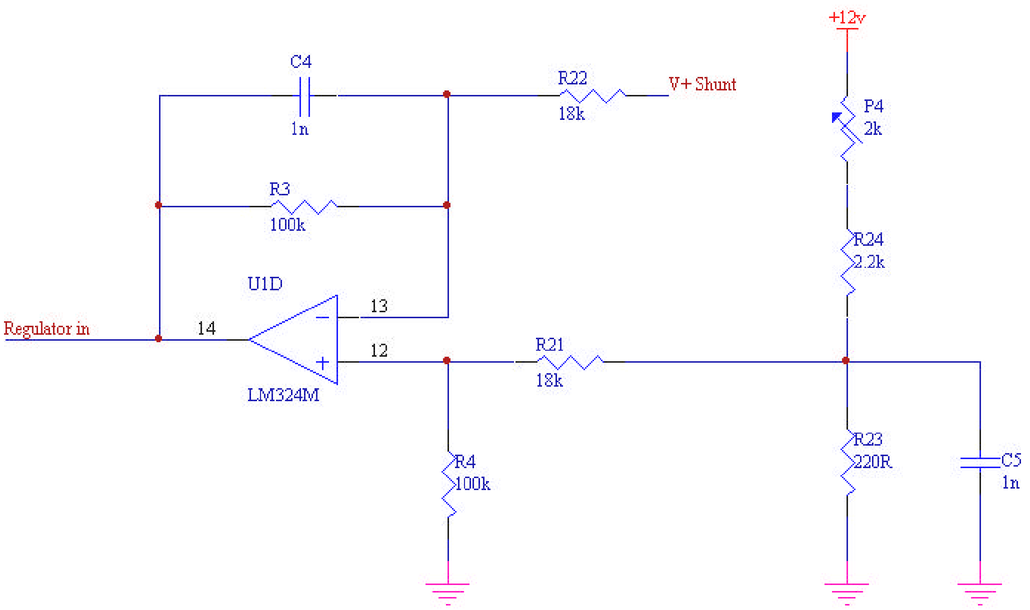

Figure 26 – Differentiator circuit

The differentiator circuitry has been designed to regulate current through the primary ignition coil from 8A down to 1.5A. As impractical as it may seem, some high-performance ignition coils may require currents in the magnitude of 8A to supply maximum spark energy and longer spark duration, ensuring complete fuel combustion. The IGBT chosen for this application is the SGP10N60, manufactured by Infineon technologies. The device is capable of handling constant currents of up to 10A at 150 degrees Celsius, it can withstand voltage levels of up to 600V, and it comes in a TO-220AB package. The output from the differential amplifier then couples to the control line input, through a series current limiting resistor, of the ignition drive circuit displayed in figure 27.

The ignition coil primary is connected to the collector of the IGBT and positive 12V rail. In case of external micro control, or if triggering from a distributor, the input, Ing Trig Sig 01, allows triggering of the ignition coil in case of a +ve 5V signal. Effectively, by supplying a +ve 5V signal to M2 gate, M2 will close circuit, forcing the gate of G1 to ground, which open circuits G1, disallowing current to flow through the device. R28 supplies a source of voltage feedback, to close the control loop of the differential amplifier in figure 26. The other circuitry to the right of the IGBT constitutes a snubber circuit and over voltage protection for the IGBT. The voltage transient suppressor diode D2, clamps at a maximum voltage of 548V across G1 so its limits are never exceeded. Please refer to Appendix D for complete data on this device. The snubber circuit of D5, C10 and R18 limits the rate of voltage rise time (dv/dt) across the IGBT, assisting in the reduction of voltage transients that appear across G1 during ignition. Please refer to Appendix A for a complete schematic diagram of the design.

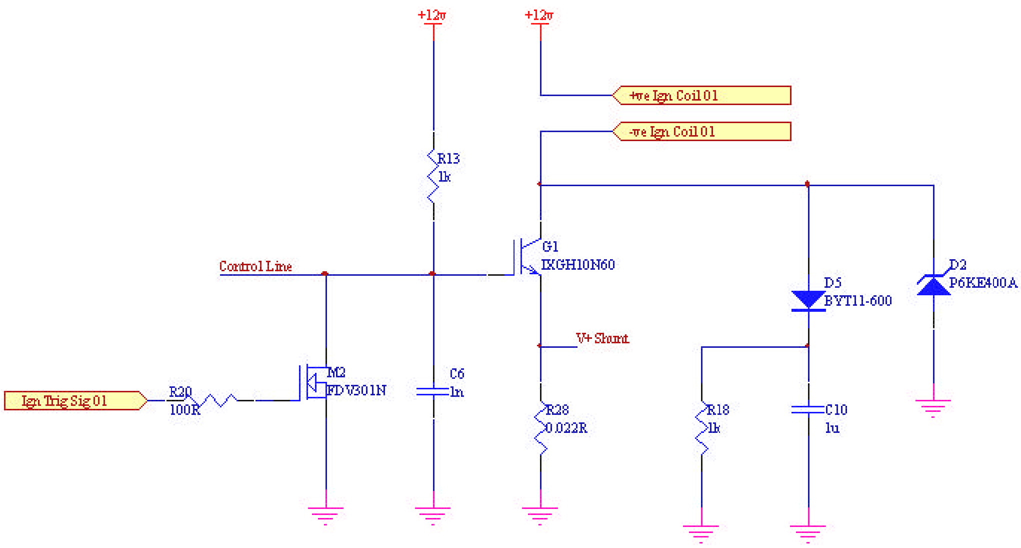

Figure 27 – Ignition drive circuit

4.22 Injector Circuit

The injector solenoid used in the project was a Bosch injector solenoid with the product inscriptions 0208 150 203. This particular injector is considered to have standard coil characteristics, not comparable to a performance solenoid. The equivalent injector coil model from figure 17 of the Bosch injector is as follows; R1 = 16.5 Ohms and L1 = 17mH. These values were obtained by inspection. The typical values for a performance injector coil are; R1 = 1 Ohms and L1 = 2mH. For this reason, the following design revolves around the worst-case scenario of the performance injector coil while providing the ability of driving the high resistance counterpart of the Bosch coil.

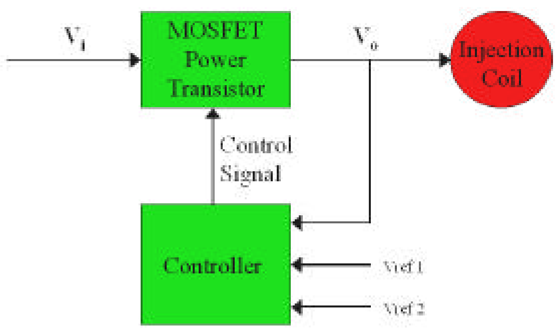

Figure 28 – Injection control loop

The control loop for the injector coil is somewhat similar to the ignition controller, with only some extra things added for the max limit level. The whole idea for the max current limit level and hold current level is to provide performance injectors with the fastest rise time response possible. This is achieved by supplying an initial higher current through the coil, so the solenoid overcomes the initial mechanically resistive force from the helical spring. Once the maximum limit is achieved and the solenoid is fully open, the controller lowers the current through the coil to a suitable holding current limit. This minimises the power dissipation through the solenoid while holding the solenoid in the on state. Both maximum and hold current limits are fully adjustable to suit every coil. The maximum current level break points are from 1A up to 5A with the hold current levels ranging from 0.5A to 4A. This provides more than enough leeway for all performance injectors, while still having the ability of servicing standard injector coils such as the Bosch injector integrated in this design.

The control block diagram in figure 28 has only one additional voltage reference of Vref2 to the diagram from that of the ignition constituent. The injector coil has less (negligible in some cases) voltage spike when the switch open circuits. Here the same switching devices were taken into consideration as for the ignition circuit. The following switching technologies were evaluated; thyristor, BJT, Darlington transistor, MOSFET and IGBT. As this controller requires the ability to limit the amount of current flowing through the device, the thyristor is automatically eliminated. As the current through the coil can reach up to 5A, the switch needs a rating of at least 5A. Ideally, a component with minimal power dissipation would be preferable, allowing smaller space restrictions. The BJT, Darlington transistor and IGBT all have a BJT final drive in common, thus restricting the devices on resistance to a higher value than that of a MOSFET. Although the BJT has better spike voltage resistance over the MOSFET, these phenomena can be reduced via appropriate snubbing and voltage transient suppressing techniques. The appropriate switching device chosen was the MOSFET, because of its lower power dissipation and higher switching speeds, with relatively similar costs.

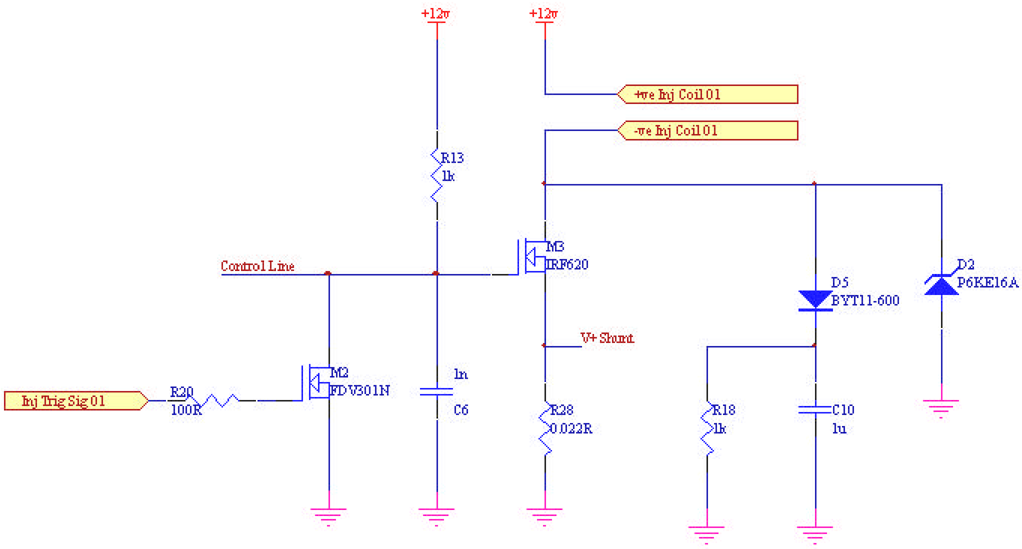

Figure 29 – Injection drive circuit

The injector drive circuit (as shown in figure 29) is identical to the ignition final drive circuit in figure 27, with only some minor component selection differences. The operation is identical, so its functionality will not be repeated here. However, the component selection of M3 and D2 is different to that of the ignition circuit. M3 is a BUZ11 MOSFET device with a 50V maximum voltage limit. This device is manufactured by ST Microelectronics, for complete data on this device please refer to Appendix D. To protect the M3 from large voltage spikes that are present during the switching off transition, the snubber circuit reduces the rate dv/dt. D2 with its maximum clamping voltage of 22.5V ensures M3 will never be damaged by over voltage spikes. The on resistance of the switching device is R_{on} = 0.03 Ohms. The corresponding conduction losses for the circuit can then be calculated. Assuming the performance model described previously to be valid and the maximum current level to be 4A with standard holding current of 1A, the initial current rise time is displayed in figure 30.

For the power loss calculation, it must be noted that this value is dependent on the input fuel pressure into the injector as this dictates, from a fluid flow perspective, the length of time the injector is required to be open. In addition, engine speed is proportional to the time the injector is needed to be held open. Ultimately, the variable that determines the fuel pressure will be the ability of the fuelling system to provide adequate amounts of fuel into the combustion chamber while the engine is operating at maximum rpm. As a guide, it is possible to calculate the maximum time the intake valve may take to inject fuel into the cylinder, assuming worst-case of 10,000rpm engine speed for a high-performance engine. The corresponding rps = 10,000/60 = 166.66rps, this is equivalent to 166.66Hz or T = 1/166.66 = 6msec.

This value of T is only for 360 degrees, so one engine cycle, or 720 degrees, is 2 x 6msec = 12msec. Now the induction cycle, from figure 2, takes ¼ of one full cycle to complete. Thus, 12msec/4 = 3msec for the induction cycle. It should be noted however, the actual time available for injecting fuel into the combustion chamber will be somewhat less than 3msec. A maximum current limit of 4A, and a hold current level of 1A were assumed. From figure 30, the time duration for the current in the coil to rise to a value of 4A is roughly 1msec, thus leaving 3-1 = 2msec in the hold state. During the hold state period the MOSFET is operating in the active region of the device. This means significant power will be dissipated through the device during this period.

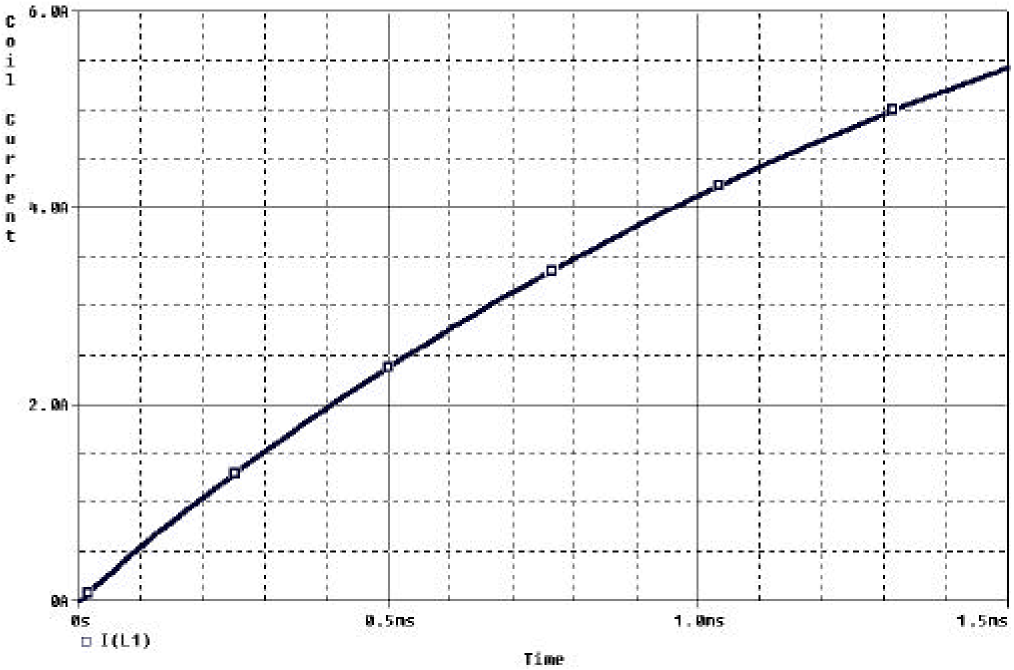

Figure 30 – Injector coil current

It is now possible to work out the power loss in the switching device. The working in this section is similar to the ignition power loss calculations and equations. The equation for power loss is P = IV(D), where D is t_{on}/t_{cycle}, the maximum rise time loss, while in the ohmic region, is P_r = (4)(0.12)(1/12) = 0.04W. The maximum conduction loss, during active region operation, is P_c = (1)(11)(2/12) = 1.833W. The 11V was determined from V = IR, if 1A current is passing through the coil, then V = IR = (1)(1) = 1V across the coil. So the MOSFET has to carry the other 12V – 1V = 11V. The total power loss of the MOSFET at 10,000rpm engine speed is $P_t = P_r + P_c$ = 0.04 + 1.833 = 1.873W, which is at absolute worse case. Again it should be mentioned, the power dissipation under normal operation would be several magnitudes smaller than the figure for continuous extreme running conditions.

The controller circuitry has the following differential amplifier, in figure 31, as the variable current hold level regulator. Here P4 is used to vary the hold current from 0.5A up to 4A. The circuit is much the same as the ignition controller circuit.

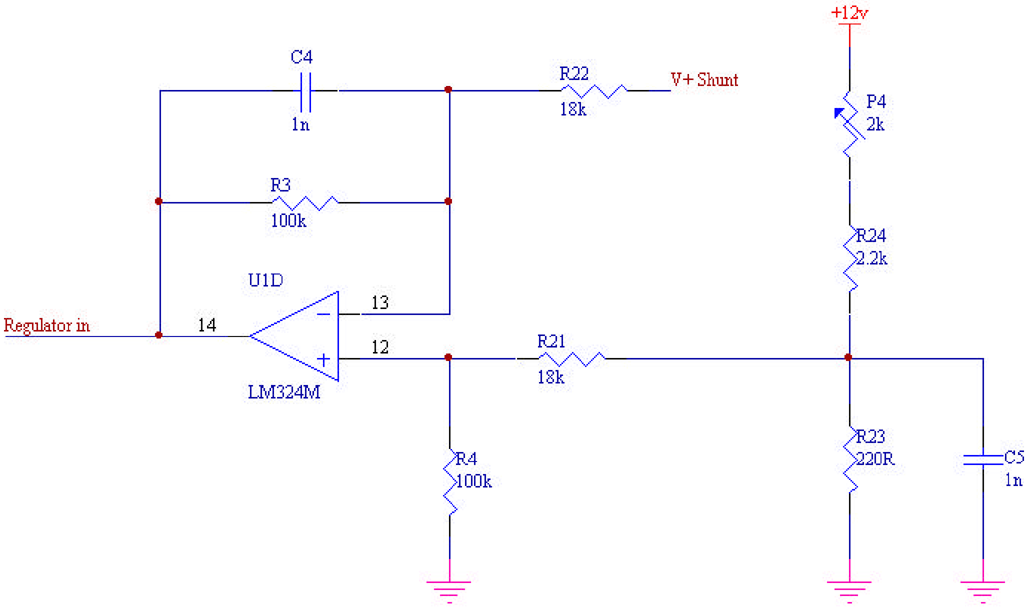

Figure 31 – Injection hold current curcuit

The two new additions to the injector controller are a maximum current limit Schmitt trigger circuit and a voltage signal amplifier-conditioner feeding into the Schmitt trigger circuitry. Firstly, the signal conditioner and non-inverting amplifier, as presented in figure 32, takes the voltage across R28 in figure 29 and amplifies it using the operational amplifier LM324. With the feedback capacitance, the output voltage spikes are reduced. The amplifier is tuned to a gain factor of 48. This signal then supplies the Schmitt trigger circuit the input signal, which controls the maximum current limit.

The Schmitt trigger circuit, portrayed in figure 33, comprises an LM324 operational amplifier and corresponding circuitry. Both P3

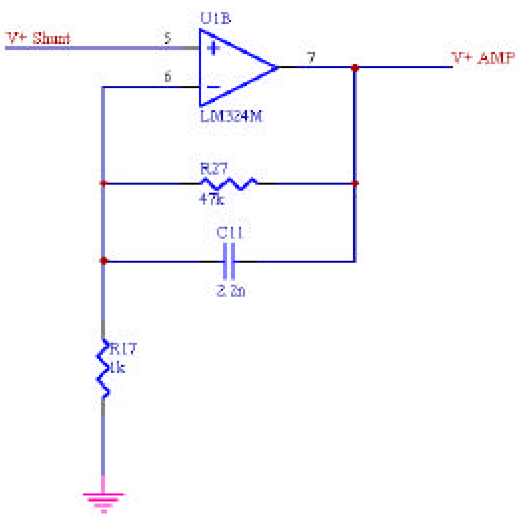

Figure 32 – Signal conditioning

and P5 together allow the adjustment of the maximum current limit value. The BJT labelled M4 is a BC807-40 surface mount device (SMD) transistor that acts as a switch which either allows or disallows the hold circuit to operate. The section that permits the initial turning on of the MOSFET M3 from figure 29 is the input of M2.

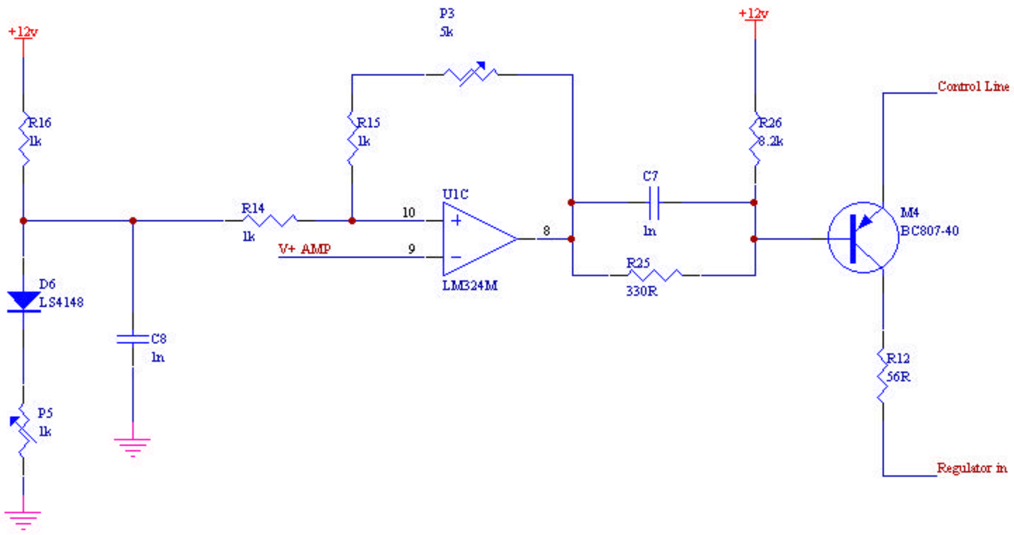

Figure 33 – Schmitt trigger circuit

Please refer to Appendix A for a complete schematic diagram of the design.

4.3 EMI Consideration for PCB Design

The effects of EMI on the control circuitry and other electrical/electronic elements in the automotive environments can be harmful to other systems. The particular issue which need addressing in high-power, fast switching designs is the particularly careful layout of components, to ensure minimal interference between modules. This includes controlling potential load dumps onto the supply rails that could severely damage or otherwise interfere with the operation of other equipment if not correctly filtered.

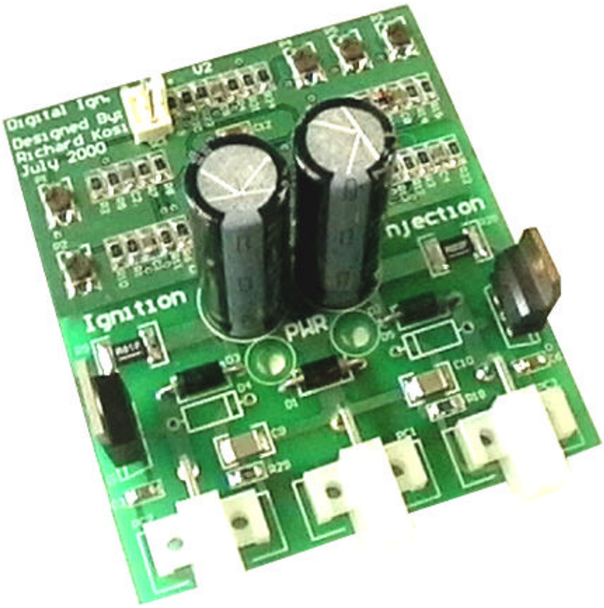

Figure 34 – Driver board

The photograph of figure 34 is the digital ignition and electronic fuel injection driver proposed in this design. SMD components were used where possible, reducing PCB size and a ground plane covers the entire control circuit layout to reduce the effects of EMI from the high power switching circuit. The ground plane can be seen from a better angle in figure 35. The ground plane is very important in designs like this, where interference in the control circuitry from external sources could cause undesirable responses to sensitive circuitry. Introducing a ground plane into the system is very important. The placing of the high power and sensitive control circuitry is a crucial issue, which has to be addressed. As evident from figure 34, the high power and control circuitry has been separated into two sections on the board. The two low impedance capacitors, towering from the board, allow the voltage rail to experience minimal voltage fluctuations that could effect other modules connected to the same power rail.

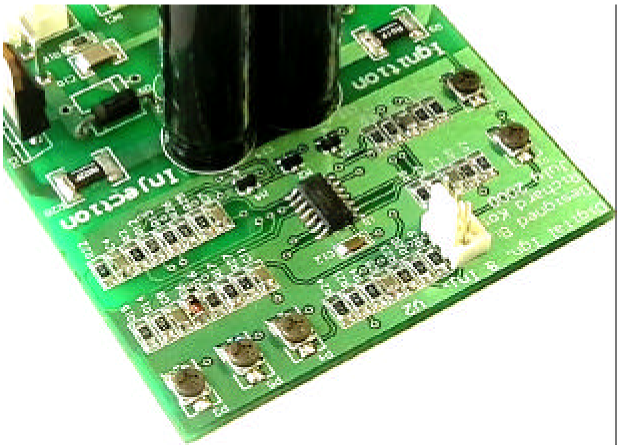

Figure 35 – Control circuitry

Track widths and track spacings are another important issue in the design of any PCB, whether it is high power, high-voltage, sensitive circuitry, or just micro components. Figure 36 is the conductor spacing chart that was used for the high power circuit layout design [13]. It is important to include such spacings for the high-voltage spikes that are incurred from the ignition and injection coil. The ignition PCB track spacing was designed for a maximum of 600V, which would need the spacing between tracks to be 120thou or 3mm apart. The injector track spacing needs to be resistant to 300V and the corresponding track width would be 50thou or 1.3mm. However, for the PCB to look aesthetically pleasing the spacing was identical to that of the ignition side.

Conductor Spacing							
Voltage Between Conductors (VDC or Peak)	Minimum Spacing (inches)						
	Bare Board				Assembly		
	B1	B2	B3	B4	A5	A6	A7
0 thru 15	0.004	0.025	0.025	0.005	0.005	0.005	0.005
16 thru 30	0.004	0.025	0.025	0.005	0.005	0.01	0.005
31 thru 50	0.004	0.025	0.025	0.005	0.005	0.015	0.005
51 thru 100	0.004	0.025	0.06	0.005	0.005	0.02	0.005
101 thru 150	0.008	0.025	0.125	0.015	0.015	0.03	0.015
151 thru 170	0.008	0.05	0.125	0.015	0.015	0.03	0.015
171 thru 250	0.008	0.05	0.25	0.015	0.015	0.03	0.015
251 thru 300	0.008	0.05	0.5	0.015	0.015	0.03	0.015
301 thru 500	0.01	0.1	0.5	0.03	0.03	0.06	0.03
More than 500	.0001 /Volt	.0002 /Volt	.001 /Volt	.00012 /Volt	.00012 /Volt	.00012 /Volt	.00012 /Volt

B1 - Internal Conductors
B2 - External Conductors, uncoated, sea level to 10,000 ft.
B3 - External Conductors, uncoated, over 10,000 ft.
B4 - External Conductors, with permanent polymer coating (soldermask).
A5 - External Conductors, with conformal coating over assembly.
A6 - External Component lead/termination, uncoated.
A7 - External Component lead/termination, with conformal coating.

Figure 36 – Conductor spacing chart

In addition, an important aspect of PCB design is the track widths for high current carrying circuits. The high power section of the circuit was designed to withstand constant currents of 8A with a temperature difference of 20 degrees from ambient temperature, this required the track width to be 130thou or 3.33mm. The injector circuit was similarly designed for temperature differences of 20 degrees Celsius however with a constant current rating of 6A, the track-width would need to be 90thou or 2.3mm in this case. Again, the actual track width was left as 3.33mm for the injector circuit for an identical appearance between the two circuits. The guidelines used for track width calculations were derived from figure 37 [13].

	Trace Width Guidelines					
	1 Oz. Plating, External Conductors					
	Width	**10°C**	**20C**	**30°C**	**45°C**	**60°C**
	.005"	400 mA	500 mA	650 mA	800 mA	1.0 A
	.010"	800 mA	1.0 A	1.3 A	1.6 A	1.9 A
Width	.015"	1.2 A	1.5 A	1.8 A	2.1 A	2.8 A
	.020"	1.5 A	1.7 A	2.0 A	2.5 A	3.1 A
	.025"	1.7 A	2.2 A	3.0 A	3.5 A	4.0 A
	.050"	3.2 A	3.9 A	4.8 A	5.7 A	6.5 A
	.100"	4.8 A	6.2 A	8.0 A	9.5 A	10.4 A
	.150"	6.0 A	8.5 A	11.0 A	12.6 A	13.5 A

Figure 37 – Track width guidline chart

Figure 38 shows the final high power PCB section design of the ignition and injection circuits. The power connectors seen towards the bottom of the board below are Mini-Fit, Jr headers manufactured by Molex. This connector can withstand voltages of up to 600V with currents up to 9 Amperes. This selection of component leaves adequate leverage for this design. To make integration to external microcontroller or distributor easy, a three-way header is supplied in the control section. Please refer to Appendix B for the complete PCB artwork of the design.

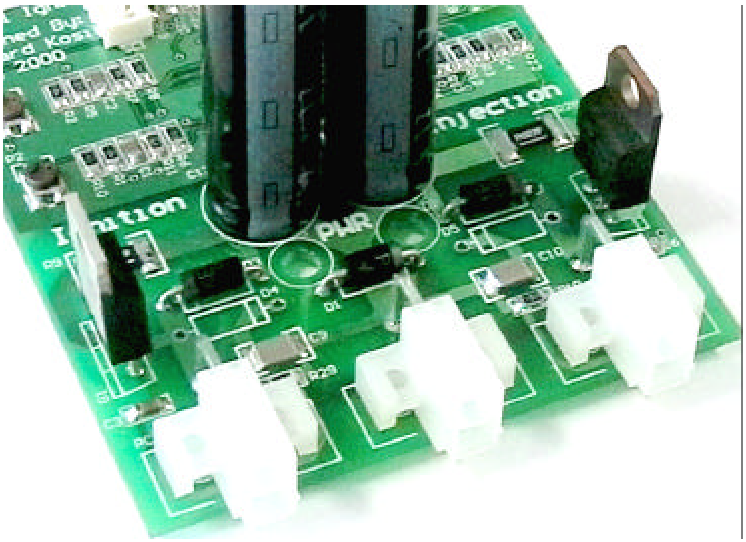

Figure 38 – Power electronics circuitry

CHAPTER 5

Software Implimentation

5.1 Software

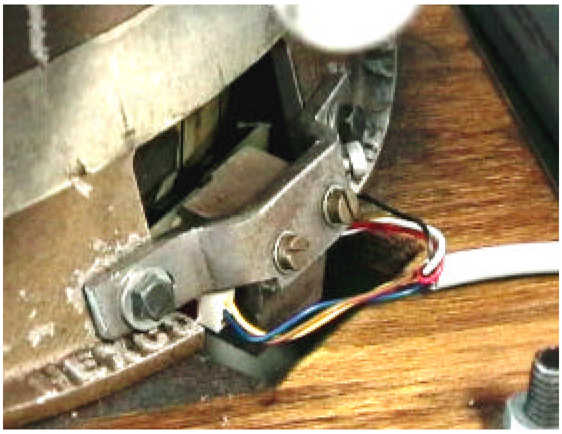

Figure 39 – Engine optical sensor

The two sensory inputs from the engine supply the M16C microcontroller with the necessary information to trigger the ignition, supplying ignition advance during higher speed operation. Figure 39 exhibits the positioning of the two optical sensors placed on the engine flywheel. Both 10 degree and 360 degree information is passed to the microcontroller for calculation of ignition timing. These signals are passed to the M16C in the form of external interrupts with their respective interrupt levels set accordingly to importance of calculation. The entire program for the M16C microcontroller was written in C-code, please refer to Appendix C for the complete program listing for the design. The different interrupt service routines (ISR's) are shown in Figure 40, below, and described in the following sections.

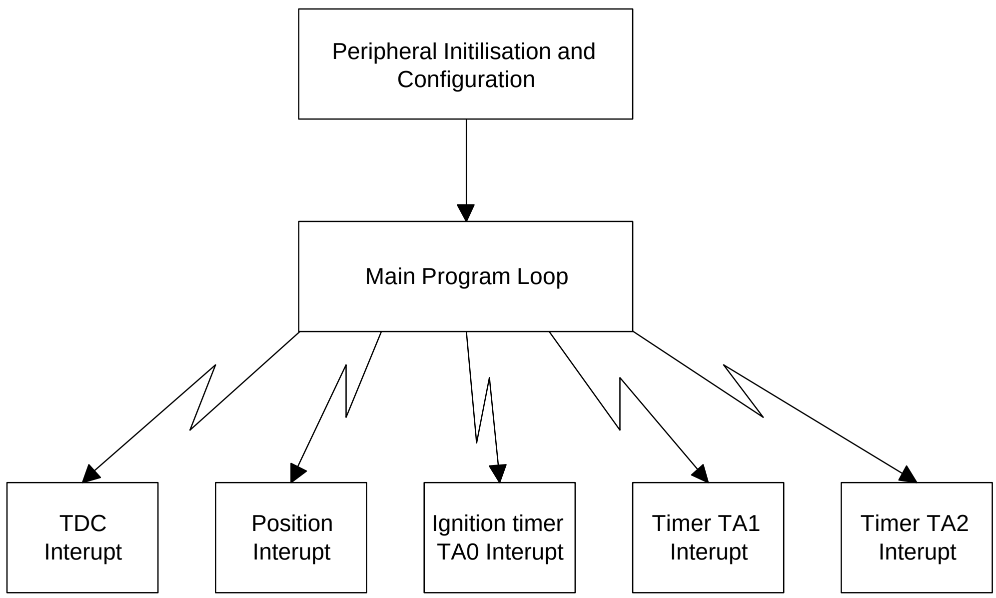

Figure 40. Program flow chart.

5.2 Peripheral Initialisation and Configuration

Several peripherals require initialisation before the program can control the ignition-timing program. Firstly, the initialisations of the I/O pins are configured, together with their corresponding internal pull-up resistors, to prevent false input states from the sensors. All the output ports are then cleared to zero.

Next, the three 16 bit timers are initialised. Timer 0 is used for the ignition coil rise time counter. It is placed in continuous counting mode and is set to down-count with 1.2msec stored in its reload register. An interrupt occurs every time counting reaches zero. The timer flag is activated, initialising counting, every 1.2msec before the ignition coil is to be triggered, thus allowing 4A current to flow through the ignition coil. Timer 1 is placed into free running counter mode and is used for calculating the average time between every 10 degrees of the flywheel rotation. The reload counter register is reset to 0xFFFF, corresponding to a maximum count of 131msec, for a frequency pre-scaling of f/32 from the main clock at 16Mhz. An interrupt is generated every time the counter reaches zero. Timer 2 is set into free running counter mode and operates as the real time base for each 360 degrees cycle. The reload register is set to 0xFFFF, equivalent to 131msec, with the system configured to automatically reload every time an interrupt occurs. The timer's interrupt levels are initialised to 3, 4, and 5 respectively before both timers 1 and 2 are activated by writing a one to their corresponding counter flag.

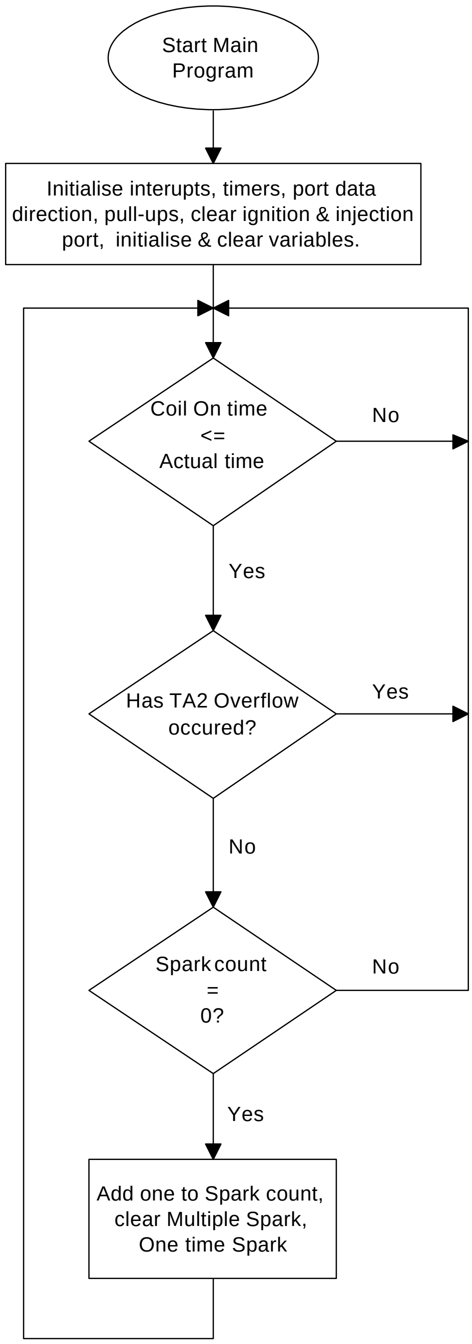

Figure 41 – Main program loop

The four external interrupts from 0 to 3 are enabled and their corresponding interrupts are set to 7, 7, 2 and 1 respectively. External interrupt 0 and 1 both service the advance or retard feature which enables the addition or subtraction of one degree from top dead centre (TDC). However, there is a programmed restriction on the amount of advance or retard that may be applied; that is from TDC, 0 degrees to 40 degrees before TDC. External interrupt 2 is connected to the optical sensor that signals every 10 degrees and external interrupt 3 is connected to the optical sensor which reports every 360 degrees of revolution.

5.3 Main Program Loop

The main program loop checks continually whether the calculated spark time equals or is smaller than the actual elapsed time from the beginning of the cycle. If this is true, the program goes on to check whether a timer overflow has occurred. If no overflow occurred during the cycle and if no other spark occurred during the current cycle, the program will branch to the subroutine 'one time spark'. The operational flow chart of the main program can be referred to in figure 41. The program loop is checked continually while not servicing ISRs or subroutines. For this reason a record of whether a spark occurred during this cycle is important to eliminate the chance of repeated sparks. However, the program is written in such a way that if the above were to happen, no spark would be induced at all. This happens as the subroutine 'one time spark' only initiates the counter flag, enabling counting of timer 0.

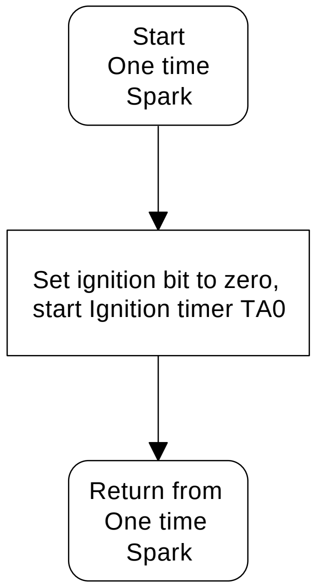

Figure 42- Subroutine spark

The subroutine 'one time spark', as exhibited in figure 42, allows the flow of current through the ignition coil via activating G1. At the same time, timer 0 initiates counting of 1.2msec and the program returns from the subroutine to the main program. The spark at the plug occurs only when the timer 0 reaches a count of zero, and it's respective ISR is serviced.

5.4 Timer A0 Interupt Service Routine (ISR)

The flow-chart for Timer A0 interrupt is portrayed in figure 43, below. To aid with fuel combustion at start-up, an extra feature has been added to the program, which supplies a dual spark, one after the other in concession until the engine speed has reached 500rpm. This feature is nevertheless serviced from the TDC interrupt only. From 500rpm upward, only one ignition spark is provided to the plug. The timer 0 ISR begins with setting the ignition bit to one, disallowing current to flow through the coil and ultimately inducing a spark across the plug. The timer is then re-initialised to the original counting value of 1.2msec or 0x01F4 in

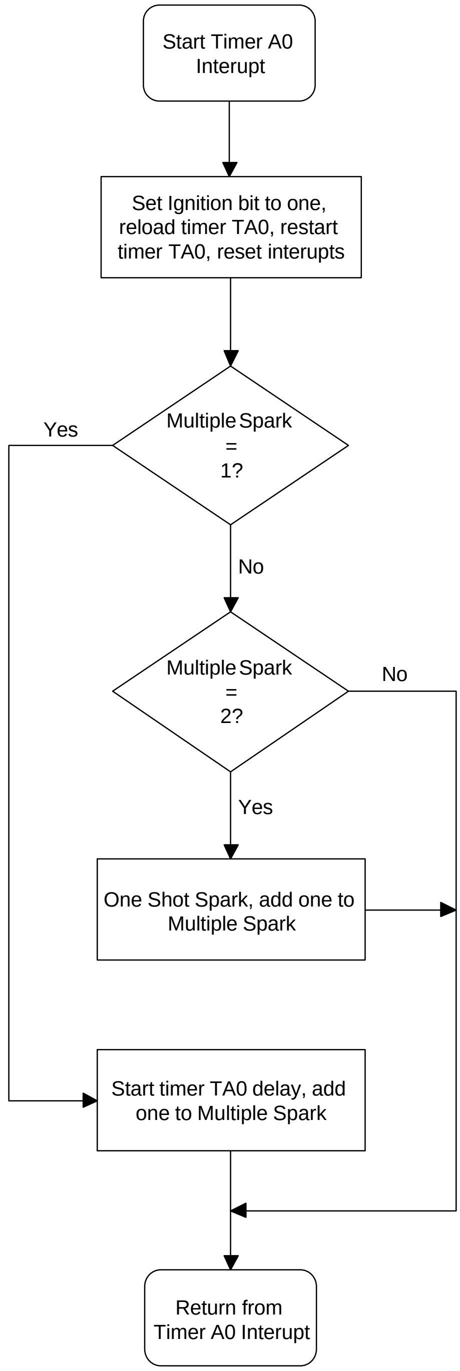

Figure 43 – TimerA0 program loop

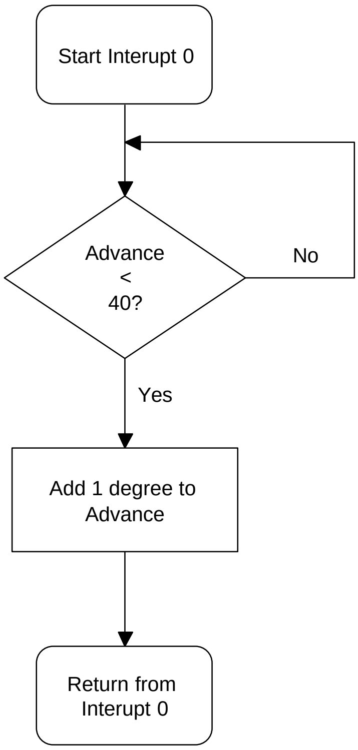

Figure 45 – Advance ISR

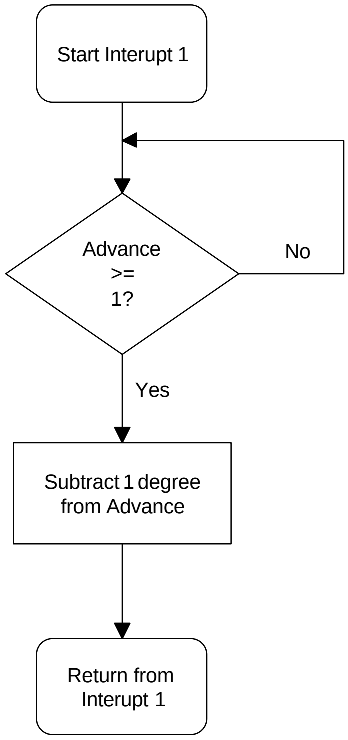

Figure 44 – Retard ISR

hexadecimal.

The program then checks if the variable multi-spark has been activated. If so, the program initialises spark counting before adding one to the variable multi-spark. Otherwise, if multiple sparking has not been selected only one spark will be activated before exiting the ISR. If the variable multi-spark is set to two then a delay of 0.5msec is activated between spark ignition, and allowing the coil to charge again.

5.5 External Interrupts

All of the external interrupts are edge triggered, so require the transitional change from logic level 0 ⇒ 1 or 1 ⇒ 0, as per configuration, to activate an interrupt service routine. There are a limited number of external interrupt sources, so programming of the microcontroller and hardware set up must be efficient. Interrupts INT0 through to INT3 were used in the program.

5.51 Advance / Retard ISR

As already mentioned, external interrupts INT0 and INT1 both service the advance and retard feature for the ignition spark control. From the development board, INT0 correlates to SW1 and INT1 correlates to SW2. The schematic for the development board may be found in the appendix. The whole purpose of the advance and retard switches is for the ability to determine easily an engine ignition map that can then be entered into the software program. This enables the user to tailor the software advance and retard amp to maximise the performance capable from their engine. Figures 44 and 45 illustrate the flow charts for these ISR. The variable advance is then used by the engine position ISR to calculate the desirable ignition point in degrees for that engine cycle.

5.52 Engine Position ISR

The engine position ISR is triggered via optical sensors every 10 degrees rotation of the flywheel. This enables the system to recalculate the idealised ignition point so that the system data is always up to date. To the right, figure 46 is the flow chart of the engine position ISR. Here the program calculates the average time over a

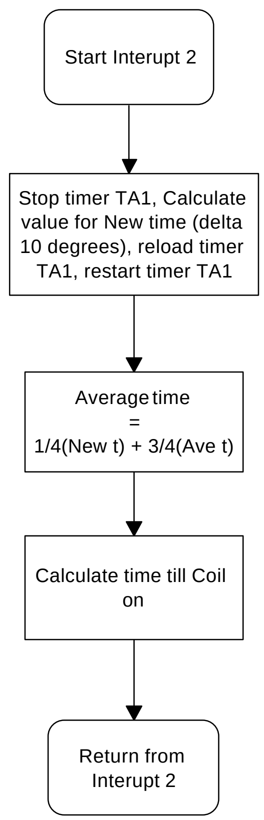

Figure 46 – Engine position ISR

span of 40 degrees. This is a working average, which means the variable gets updated every 10 degrees. The average time is with respect to 10 degrees of rotation. This system calculates the spark time over a 360 degree span. The ignition would normally be at the end of every half a cycle or 360 degrees, due to lack of sensory data. The calculation then becomes ⇒ spark time = [(360 – advance) x (average time)]/10, from this the coil start time can be calculated ⇒ coil time = spark time – 1.2msec. The coil time is then the time, with reference to the last TDC, at which current should be allowed to flow through the coil for ignition to occur another 1.2msec after activation.

5.53 Engine TDC ISR

The TDC ISR's main function is to re-initialise TimerA2, which is used as a real time reference for the 'actual time', in the main program loop, figure 47. The main programming issue here was the complications that could arise if the engine is in the starting phase, while the engine speed may be lower than 500rpm. The time that would elapse during this engine speed is 120msec, for 360 degrees of revolution. The timers maximal timing capacity is 131msec. Before the timer overflows, a suitable method for handling the overlap transition from starting and running needs to be addressed. A valid starting method proposed for this design, was to check for the occurrence of a spark in the elapsed

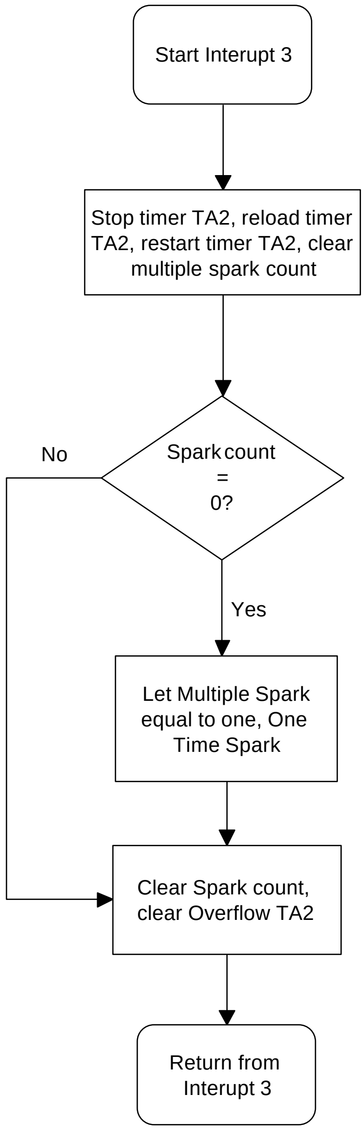

Figure 47 – Engine TDC ISR

cycle. If no spark occurred and TimerA2 had overflowed, then it can be presumed the engine is in the starting phase, or below 500rpm, in which case multiple sparking is activated and the first ignition take place 1.2msec after TDC, followed by another spark 1.7msec later. The spark variable is then reset to zero and the overflow count for TimerA2 is cleared.

5.6 Programming the Microcontroller

The M16C evaluation board comes with its own C compiler and download program from Mitsubishi. After compiling the C program the .x30 target file can be downloaded to controller via the Windows-run KD30 software program. Downloading the compiled C code is done across a DB-9 serial link to the development board. On completion of downloading the C program, the microcontroller requires resetting before the controller can be run. During any period the controller board is not running, power to the driver board must be cut to prevent burning of the MOSFET and IGBT. Their inputs are prone to floating which can lead to the ramping of current through the ignition and injector coil. The pull-up resistors that are a feature built into the microcontroller, are disabled while power down.

CHAPTER 6

Project Testing and Design Evaluation

6.1 Hardware Performance

The hardware performance is conceptually good with all the simulations closely correlating to the real world results. The PSPICE simulation data was performed over a temperature ranging between –40 degrees Celsius to +150 degrees Celsius, providing stability across the complete range. Practical testing was, however, limited to room temperature. As the operational amplifier and MOSFET devices have considerably good tolerance to temperature difference, I perceive the simulation results will prove to be realistic for different temperatures in the real world.

The effects of dual ignition during the starting phase, as discussed in the programming section, can be viewed in figure 48. Both of the waveforms labelled (1) and (2), are the signals received from the optical sensor. Waveform (1) corresponds to 10 degrees of rotation, and (2) is the TDC signal.

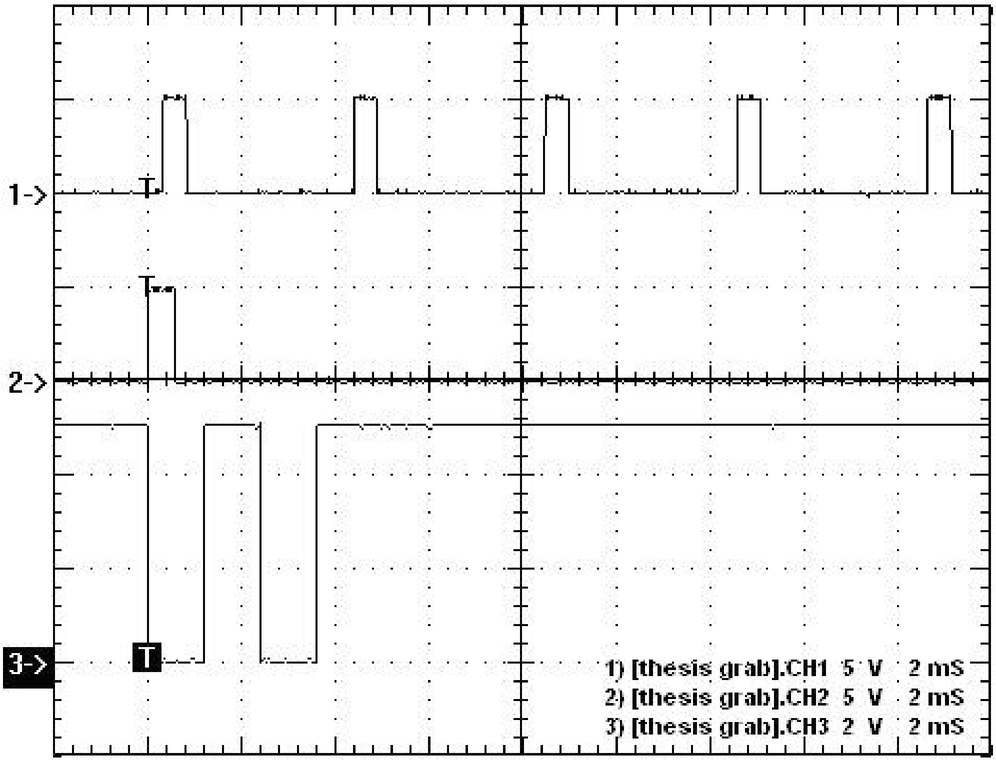

Figure 48 – Dual ignition concept

The waveform marked with (3) is the ignition drive signal. A logic of '1' corresponds to the IGBT being open circuited, inversely if the signal has a logic '0' then the IGBT is closed circuited, allowing current to flow through the coil. In total a time span of 2.4msec is necessary between spark occurrence. This allows the coil harmonics to settle after triggering, and energise the coil a second time.

6.11 Ignition Circuit

The simulations that were carried out through the aid of PSPICE for the ignition circuit showed confidence of successful operation. The current waveform, once set to regulate at 4A, levelled out quite nicely to store 20mJ of energy in the core of the ignition coil. To test the ignition circuit a 5V square wave input signal with a period of 6msec was connected to the ignition driver input. The PSPICE simulated current waveform through the coil is displayed in figure 49, below. The consistent temperature range that was used for all simulations is in the following order; -40°C, 0°C, 27°C, 100°C and 150°C consecutively.

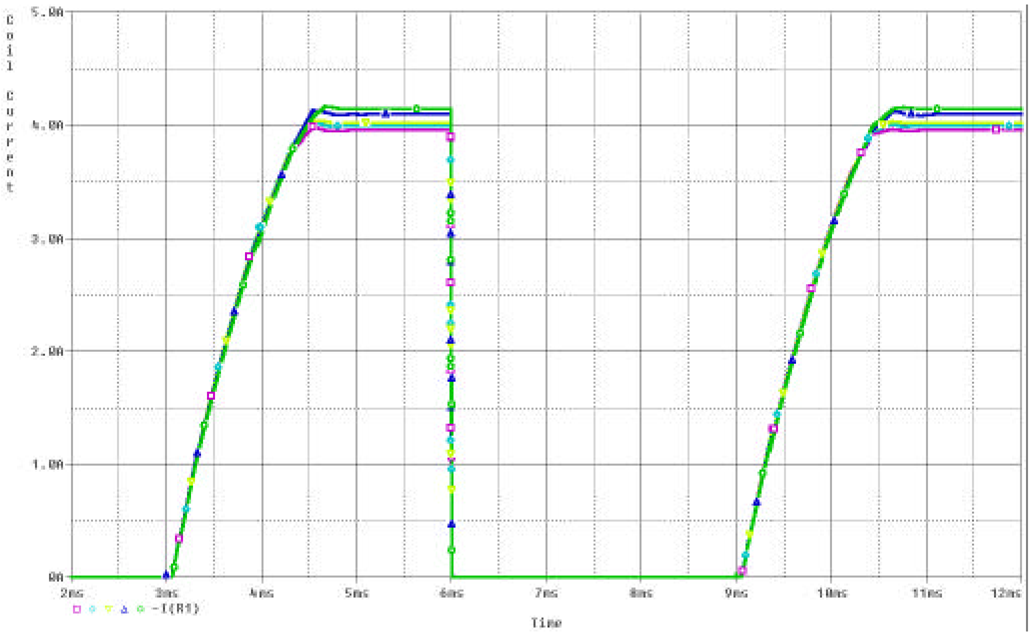

Figure 49 – Ignition coil current over Dtemp

This reinforces the design being strongly resistant to temperature change and able to be used in an automotive environment. The overshoot in the current waveform is considerably negligible, <5%, showing the controller has good characteristics, comparable to a finely tuned control loop.

The voltage spike induced across the IGBT during ignition can reach dangerous levels if not effectively suppressed. However, there is an inversely proportional ratio between the amount of suppression applied and the voltage at the spark plug. There has to be a compromise to the amount of suppression, which is acceptable. Pushing the IGBT to its upper limits is not always desirable, yet setting the spike to ¾ the IGBT's limit is quite acceptable for continuous operation. Thus, voltage levels of around 450V under normal operational conditions are favourable. Figure 50 illustrates the voltage spikes simulated in PSPICE with voltage levels in the order of that mentioned above.

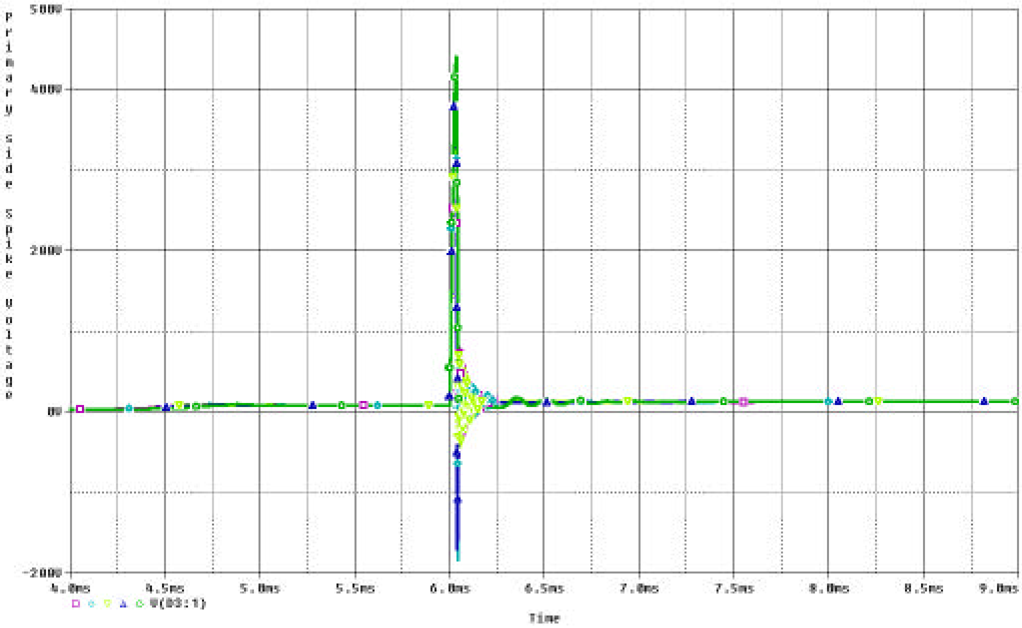

Figure 50 – Ignition IGBT voltage over Dtemp

The actual voltage at the IGBT, in figure 51, during a spike occurrence, closely correlates to the simulated version in figure 50, above. Close inspection indicates the maximum primary coil spike voltage to be at ≈450V. In both the simulated and actual graphs, this level is acceptable for continuous operational mode of the ignition circuit. This reinforces the importance of the snubber and suppression circuitry, and the effect they have on constraining the voltages across the IGBT to conservative levels, which ensure the life of the device.

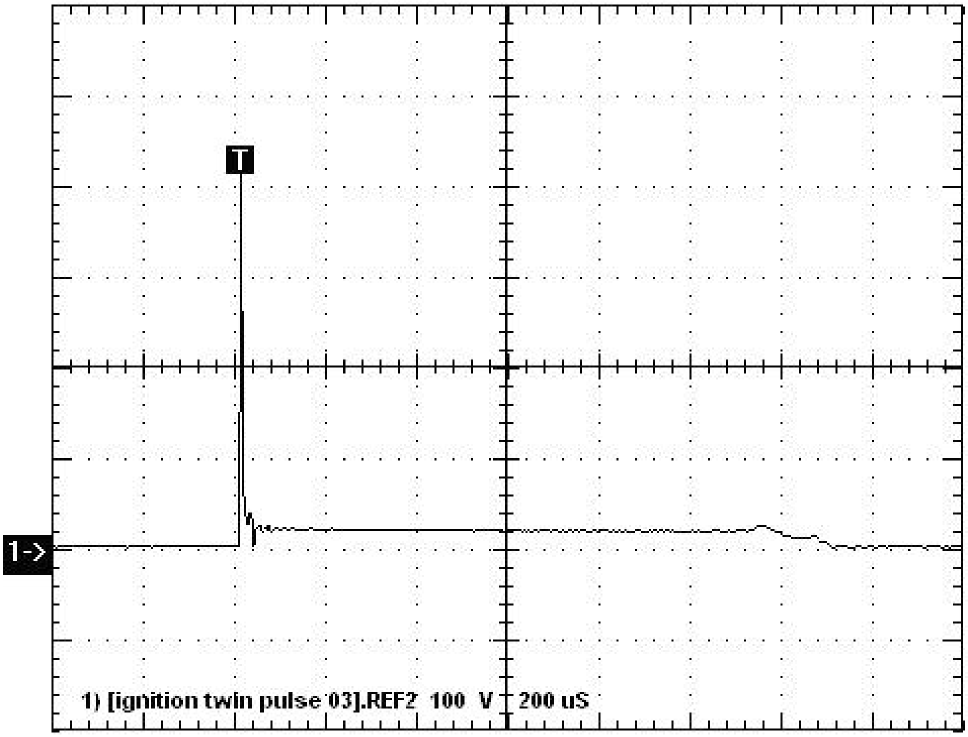

Figure 51 – Ignition IGBT voltage at T =27°C

6.12 Injection Circuit

The injector circuit was configured to have an upper current limit of 4A and a hold current limit of 1A. The test configuration that was implemented on the injector driver circuitry was a 5V square wave with signal period of 6msec. This signal was passed to the input on the injection driver. The current waveform simulated in PSPICE is displayed in figure 52. The upper limit Schmitt trigger circuit controller shows little resilience to temperature variation, though the hold current circuitry exhibits some large deviations in steady state current with the fluctuation in temperature. The variation in steady state hold current can be traced back to the BJT used in the control loop circuitry. BJT devices are strongly affected to temperature change. The device could possibly be substituted with a low voltage MOSFET transistor with similar current characteristics to avoid the undesirable (yet tolerable) response.

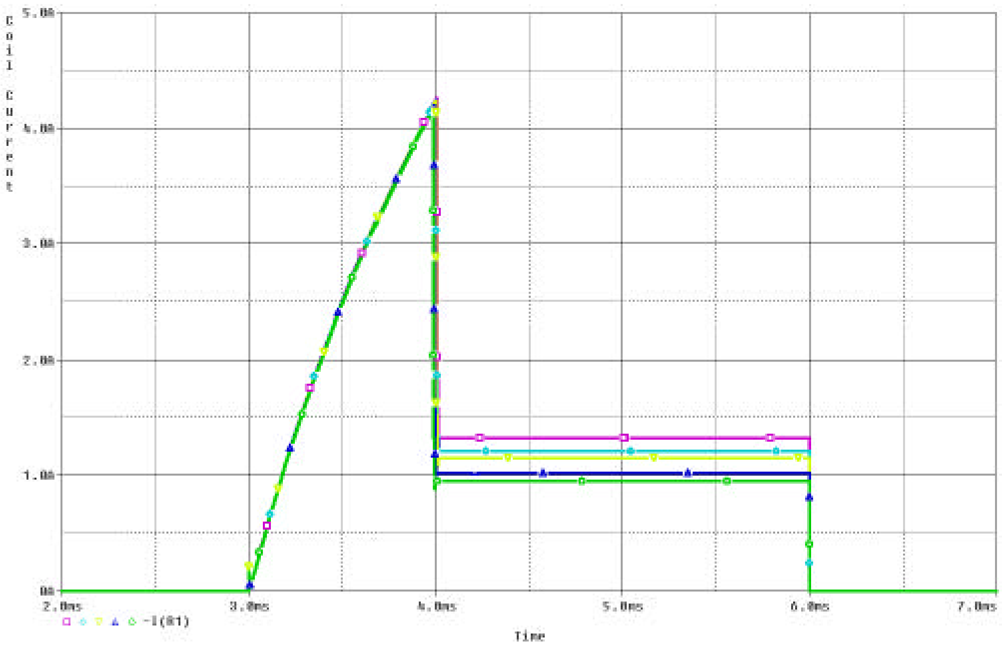

Figure 52 – Injector coil current over Dtemp

On the other hand, the voltage suppression of the injection circuit is handled very well, with voltage surges reaching no more than 60V in PSPICE simulations. The simulation results can be seen in figure 53.

The first large voltage spike at 4msec corresponds to the reduction in coil current from 4A to 1A. Once the maximum current limit is reached, the current through the coil is reduced to a holding current level. The final voltage spike relates to the holding current being ceased and the injector closing the valve. The larger the reduction in current through the coil as well as the di/dt rate associates proportionally with the size of the voltage spike across the MOSFET switching device.

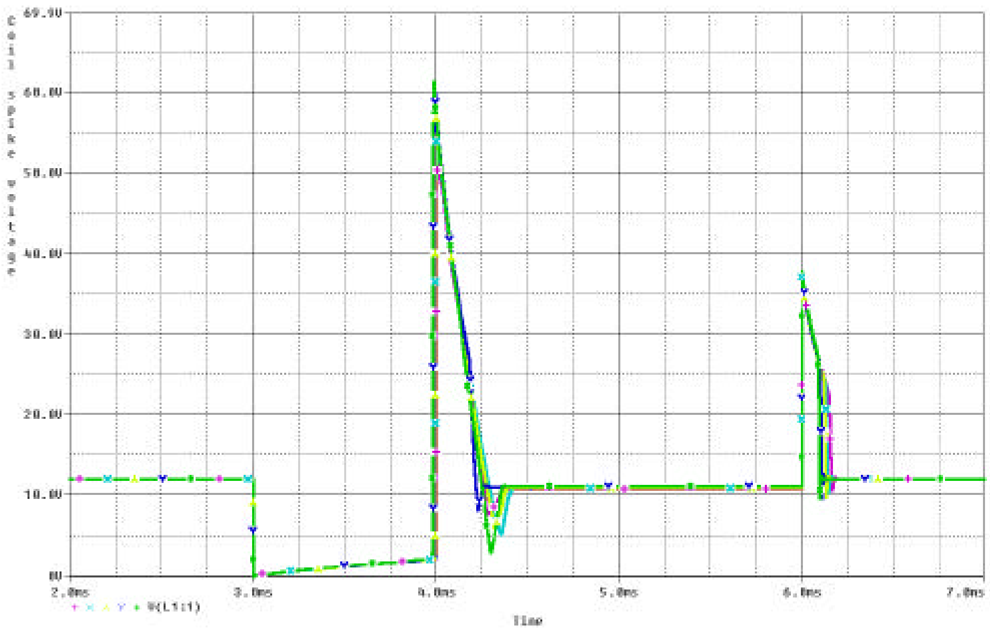

Figure 53 – Injector MOSFET voltage over Dtemp

6.2 Software Performance

Although no extravagantly involved or complicated coding was included into this project the software operated efficiently and most importantly correctly as planned. The complete software code was written in C code. The reason behind this was the easy readability of the program as in comparison to assembler code. In addition, the C code could be generated at a faster rate then that of tedious assembler code. The most important thing in any project is whether the program does what the requirements specified. This is exactly what this program does.

6.3 Project Downfalls

The stresses of this project set in during the sudden departure from the software programmer at the end of the first semester. This has set back the project's initial goal of a complete 'engine management system' to just 'digital ignition and electronic fuel injection'. The workload of the initial goal was too involved for only one thesis student, as both software and hardware were to be developed. The project continued with the development of hardware and software, however on a slightly smaller scale then initially sought.

The project suffered no other major problems. Nevertheless, the above predicament set the project back further than was initially imagined.

CHAPTER 7

Conclusions and Recommendations

7.1 Conclusion

This project was entirely successful in its aim of producing the hardware for a modern digital ignition and electronic fuel injection control system for the VTE-2 VISI-Trainer Engine. More work is needed on the software before the engine controller can be used with a complete engine ignition map for high-performance operation. The task of designing and implementing an optimal controller for this engine is not a small one, and could easily be the subject of another thesis. Although the ignition and injection driver hardware was only built to service a single cylinder engine, there is no difficulty in rearranging the components to produce a PCB that will service a multiple cylinder engine. However, the controller software would require minimal alteration to compensate for this.

7.2 Future Work

Internal combustion engines will still be used as a primary mover of automobiles until such time a more efficient and environmentally friendly power plant, suitable for mass production, is introduced into the industry. Until such time, the further development of the IC engine, improving its efficiency, response characteristics and effect on the environment is crucial if the IC engine is to stay ahead of fully electric or hybrid vehicles. Further work on this project may include:

- Mechanically integrating the fuel injector to an induction manifold on the engine.

- Software may be developed to include a digital ignition map of the engine and provide closed loop fuelling feed back control using a lambda sensor .

- Knock control could be added as an extra feature, ensuring longer life of the mechanical components of the engine.

- A separate controller board using the M16C could be designed to encapsulate the features mentioned above, with the inclusion of other technologies, such as variable valve timing (VVT), that may be added to the hardware for future integration.

References

[1] M. Gallagher, "The XK8 engine management system and electronic engine control module," *IEE Colloquium on The Electrical System of the Jaguar XK8*, IEE, London, UK, 1996, pp. 1/1-13.

[2] P.D. Jordan, "Microprocessor-controlled engine management," *Electronics-&-Wireless-World*, Vol. 90, No. 1622, Sep. 1987, pp. 876-880.

[3] P.D. Jordan, "Advanced engine management systems," *Electronics-&-Wireless-World*, Vol. 93, No. 1622, Dec. 1987, pp. 1225-8.

[4] H.A. Kuck, H.D. Erdmann, and M. Lowel, "The knock detection of Volkswagen's supercharged 1.3 L SI-Engine," *Sixth International Conference on Automotive Electronics*, IEE, London, UK, pp.70-76.

[5] L. Simpson, R. De-Jong, "Transistor-assisted ignition system with dwell extension and full protection," *Electronics-Australia*, Vol. 41, No. 9, Dec. 1979, pp. 60-3, 65-6.

[6] A. Beer, A. Cypra, "Gasoline Fuel-Injection System L-Jetronic," *Robert Bosch GmbH, Automotive Equipment Business Sector,* Stuttgart, 1997.

[7] A. Beer, A. Cypra, "Ignition," *Robert Bosch GmbH, Automotive Equipment Business Sector,* Stuttgart, 1999.

[8] J.L. Lumley, *Engines An Introduction,* Cambridge University Press, Cambridge, 1999.

[9] T. Wakabayashi, H. Mitomo, A. Kida, Y. Ikeya, "Electronic control ignition for 2-wheeled vehicles," *Oki-Technical-Review,* Vol. 57, No. 139, July 1991, pp. 1-4.

[10] T. Kattwinkel, “16-bit microcontroller C167R with full-CAN module: tuning up automotive networks with the CAN bus,” *Siemens-Components*, Vol. 30, No. 6, Nov.-Dec. 1995, pp. 18-20.

[11] EFI 332 engine management system development, http://efi332.eng.ohio-state.edu/efi332/

[12] J. Clarke, “Universal High Energy Ignition System,” *Silicon Chip*, Vol. 11, No. 6, June. 1998, pp. 18-27.

[13] G. Patrick, Praegitzer Industries, http://www.aracnet.com/~gpatrick/welcome.html

[14] ACDelco, http://www.acdelco.com/parts/tech/1530b.htm

Appendix A – Schematic Diagrams

A.1 – Digital Ignition and Electronic Fuel Injector Driver

Appendix B – PCB layers

B.1 – Digital Ignition and Electronic Fuel Injector Driver

Appendix C – Programe C-code Listing

C.1 – Motor3.c

Appendix D – Discrete Component Data

D.1 – MOSFET Data

D.2 – IGBT Data

D.3 – BJT Data

D.4 – Diode Data

Appendix E – Integrated Semiconductor Data

E.1 – M16C Microcontroller Data

E.2 – LM324M Operational Amplifier Data